Summer 8-15-2016

Spectral Properties of Fractional Quantum Hall Hamiltonians

Amila Weerasinghe
Washington University in St. Louis

WASHINGTON UNIVERSITY IN ST. LOUIS

Department of Physics

Dissertation Examination Committee:
Alexander Seidel, Chair
Renato Feres
Zohar Nussinov
Michael C. Ogilivie
Stuart A. Solin
Li Yang

Spectral Properties of Fractional Quantum Hall Hamiltonians

by

Amila Weerasinghe

A dissertation presented to the
Graduate School of Arts & Sciences
of Washington University in
partial fulfillment of the
requirements for the degree of
Doctor of Philosophy

August 2016
St. Louis, Missouri

TABLE OF CONTENTS

Page

List of Figures iii

List of Tables v

Acknowledgments vi

Abstract of the Dissertation viii

Chapter 1: Introduction 1
1.1 Quantum Hall Effect 1
1.2 Understanding the Fractional Quantum Hall Effect 15
1.3 Motivation 23
1.4 Outline of the Thesis 26

Chapter 2: Thin torus perturbative analysislavin of elementary excitations in the Gaffnian and Haldane-Rezayi quantum Hall states 28
2.1 Gapless Excitations in the Haldane-Rezayi state 30
2.2 Thin torus elementary excitations in the Gaffnian state. 40
2.3 Discussion and Conclusion 57

Chapter 3: Bounds for low-energy spectral properties of center-of-mass conserving positive two-body interactions 59
3.1 Monotony of Ground State Energy 61
3.2 Specialization to center-of-mass conserving Hamiltonians 66
3.3 Discussion and Conclusion 90

Bibliography 92

LIST OF FIGURES

Figure Number — Page

1.1 Schematic diagram of the Hall experiment. The current I and the external magnetic field B are perpendicular to each other. This gives rise to the Hall Voltage V_H perpendicular to the direction of the current flow. 2

1.2 Change in Hall voltage U_H and the voltage drop between the recording probes U_{pp} in a constant magnetic field 18 T with respect to the gate voltage V_g. Figure is taken from Ref.[8] with permission. 4

1.3 Lowest Landau level single-particle states in a disk (symmetric gauge in planar geometry). The radius of a circle is given by, $r = \sqrt{2m} l_B$ 9

1.4 Lowest Landau level single-particle states in the cylinder geometry with circumference L_y. Lines depict the highest probability location of the lowest Landau level orbitals. Periodic boundary conditions are implemented in the y-direction. The x positions (guiding centers) are at, $X_m = m\,\kappa\, l_B^2$. 11

1.5 (a) Sharp Landau levels in the absence of disorder (b) In the presence of disorder, Landau levels are broadened into bands of extended and localized states. 14

1.6 Hall resistance R_H and the longitudinal resistance R as a function of magnetic field. The dashed diagonal line represents the classically expected variation. Plateaus of R_H appear in the integer and fractional values corresponding to IQHE and FQHE respectively. R is minimum at the plateaus. Figure is taken from Ref.[24] with permission. 16

2.1 Haldane-Rezayi thin torus ground state patterns, in the usual occupation number representation. Zeros denote empty orbitals. The configuration $\uparrow\downarrow$ denotes an up-spin and a down-spin particle occupying the same orbital. Ovals denote spin singlets. 30

2.2 The thin torus limit of a particular ground state of the hollow core Hamiltonian. The limiting form is an equal amplitude superposition of states with a delocalized pair of charge-neutral defects forming a singlet. 31

2.3 A spin-1/2 deffect becomes delocalized in an A-type ground state pattern . . 34

2.4 The off-diagonal matrix element delocalizing spin-1/2 defects. 38

2.5 Comparison between the gap according to Eq. (2.40) (solid line) and numerical work(dots), for 8 and 10 particles. The Hamiltonian parameter C, Eq. (2.17), has been set equal to 1. We have obtained qualitatively similar results for different values of C. 55

2.6 Checking the relative strength of the terms in the denominator of the gap Eq. (2.40) for different C values. Linear fit (solid line) gives an intercept and gradient of 9.0046 and 1.0006 respectively, which is in good agreement with Eq. (2.40). 56

3.1 Schematic variation of ground state energy of a "special" Hamiltonian according to the knowledge prior to the current project. Nothing much is rigorously known in the region shown in purple (dashed line). L is the number of lowest Landau level orbitals available. Ground state energy is zero until N_I ("incompressible particle number") which is $L/3$ for Laughlin 1/3 state. 78

3.2 Schematic variation of ground state energy of a "special" Hamiltonian. Upper bounds for the "charge gap" and energy step size (at black dots) for the ground state energy and the first excited state energy has been proved. L is the number of lowest Landau level orbitals available. Ground state energy is zero until N_I ("incompressible particle number") which is $L/3$ for Laughlin 1/3 state. 83

LIST OF TABLES

Table Number Page

2.1 The Number of particles in a cluster $(g+1)$, and the angular momentum projection, $L_{g+1} < L_{g+1}^{min} + p$ for different quantum Hall states. 43

3.1 Charge gap for a sphere threaded by $N_\Phi = L - 1$ flux quanta, at the incompressible filling factor of the V_1 Haldane pseudopotential (see text). N represents particle number, the parameter Δ defined by Eq. (3.42) equals $1-3/(2L)$ for the V_1 pseudopotential, $(\Delta_c)_{ub}$ is the upper bound on the charge gap as given by Eq. (3.52), and $(\Delta_c)_{ED}$ is the actual charge gap as determined by exact diagonalization. 86

ACKNOWLEDGMENTS

I am grateful to all the teachers I came across in my life as they have provided great opportunities for me to acquire needed knowledge. They are the ones along with my parents who have shaped me up to be the person that I am today. I am thankful to all the institutions such as Washington University in St. Louis, University of Peradeniya, Kingswood College Kandy and Medirigiriya National School for providing me free education so far in my life.

I am utterly grateful to my thesis advisor, Prof. Alexander Seidel for his valuable guidance and support during last five years. He was always patient with me and guided me in the correct path so that this thesis became a reality. His support was in so many different levels ranging from guidance in the research to taking life changing decisions, and he always directed me to be better. Moreover, I thank my mentors, professors Zohar Nussinov and Stuart A. Solin and the other PhD committee members, professors Michael C. Ogilivie, Li Yang and Renato Feres.

My mother, late father, two sisters and wife are the true owners of my achievements. I am grateful to them for bearing with me, for all the encouragements in tough times and for making an easy and pleasant atmosphere to do my studies. I am grateful to my wife, Waruni for the great emotional support she gave to me. Last but not least, I thank my group members, other friends and colleagues and the non-academic staff members of the physics department for making my time at Washington University a pleasant one.

DEDICATION

to my family

ABSTRACT OF THE DISSERTATION

Spectral Properties of Fractional Quantum Hall Hamiltonians

by

Amila Weerasinghe

Doctor of Philosophy in Physics

Washington University in St. Louis, 2016

Professor Alexander Seidel, Chair

The fractional quantum Hall (FQH) effect plays a prominent role in the study of topological phases of matter and of strongly correlated electron systems in general. FQH systems have been demonstrated to show many interesting novel properties such as fractional charges, and are believed to harbor even more intriguing phenomena such as fractional statistics. However, there remain many interesting questions to be addressed in this regime. The work reported in this thesis aims to push the envelope of our understanding of the low-energy properties of FQH states using microscopic principles.

In the first part of the thesis, we present a systematic perturbative approach to study excitations in the thin cylinder/torus limit of the quantum Hall states. The approach is applied to the Haldane-Rezayi and Gaffnian quantum Hall states, which are both expected to have gapless excitations in the usual two-dimensional thermodynamic limit. For the Haldane-

Rezayi state, we confirm that gapless excitations are present also in the "one-dimensional" thermodynamic limit of an infinite thin cylinder, in agreement with earlier considerations based on the wave functions alone. In contrast, we identify the lowest excitations of the Gaffnian state in the thin cylinder limit, and conclude that they are gapped, using a combination of perturbative and numerical means. We discuss possible scenarios for the cross-over between the two-dimensional and the one-dimensional thermodynamic limit in this case.

In the second part of the thesis, we study the low energy spectral properties of positive center-of-mass conserving two-body Hamiltonians as they arise in models of FQH states. Starting from the observation that positive many-body Hamiltonians must have ground state energies that increase monotonously in particle number, we explore what general additional constraints can be obtained for two-body interactions with "center-of-mass conservation" symmetry, both in the presence and absence of particle-hole symmetry. We find general bounds that constrain the evolution of the ground state energy with particle number, and in particular constrain the chemical potential at $T = 0$. Special attention is given to Hamiltonians with zero modes, in which case similar bounds on the first excited state are also obtained, using a duality property. In this case, in particular an upper bound on the charge gap is also obtained. We further comment on center-of-mass and relative-decomposition in disk geometry within the framework of second quantization.

Chapter 1

INTRODUCTION

Condensed matter physics is instrumental in understanding the immediate physical world around us. It is a sub-area of physics that has frequently seen drastic paradigm changes of our existing knowledge. New experimental discoveries in this area of physics often urged for new physical ideas demanding fundamental changes to pre-existing notions. The research presented in this thesis concerns a branch of condensed matter physics that has been a driving factor for paradigm change over the last few decades, namely that of fractional quantum Hall (FQH) systems. In this thesis, we aim to investigate the (low-energy) spectral properties of FQH systems modeled by microscopic Hamiltonians, mostly by analytic means. In the following we give a brief introduction to the physics of quantum Hall systems leading up to the main motivations for the work reported in later chapters. More detailed introductions can be found elsewhere [1–3].

1.1 Quantum Hall Effect

In 1879, while investigating a side note made by Maxwell, E.H. Hall [4] discovered that, in the presence of a magnetic field and a current, a voltage difference occurs perpendicular to both the applied magnetic field and the current. This is called the Hall effect. The Hall voltage has a classical origin. The electrons moving in a magnetic field feel the Lorentz force

which produces a drift in the direction perpendicular to the traveling direction. This leads to a voltage difference perpendicular to the external field. Using the Ohm's law, a non-dissipative resistance can be associated with this voltage, which is called the Hall resistance. Hall resistivity can be proved to be,

$$\rho_H = \frac{B}{\rho q c} \ , \tag{1.1}$$

where ρ is the density of electrons, B is the magnetic field strength, q and c are the charge and speed of light respectively. It is clear that the Hall resistivity is directly proportional to B. This behavior can be utilized to determine the carrier charge density ρ and the type of carriers.

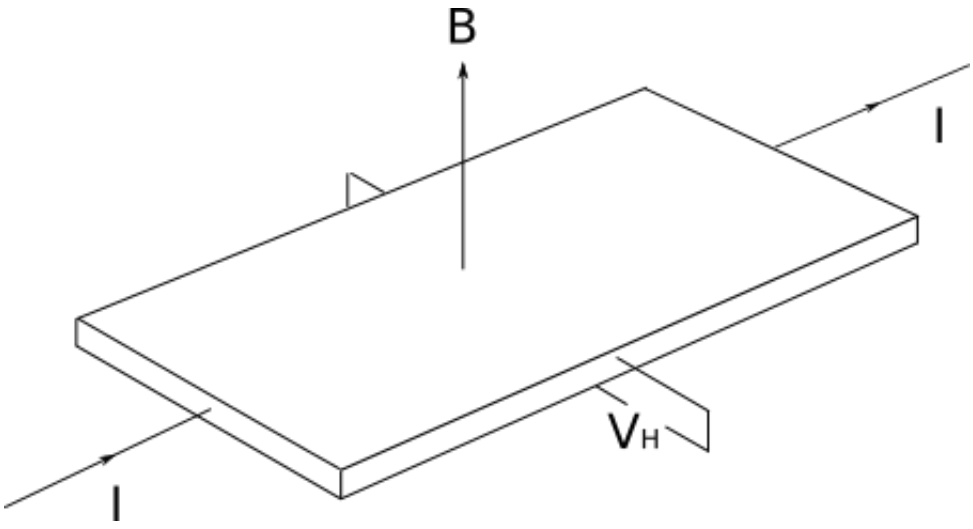

Figure 1.1: Schematic diagram of the Hall experiment. The current I and the external magnetic field B are perpendicular to each other. This gives rise to the Hall Voltage V_H perpendicular to the direction of the current flow.

1.1.1 Integer Quantum Hall Effect

When electrons are confined to two dimensions (in three-dimensional space) in considerably clean samples, cooled down to very low temperatures and subjected to high magnetic fields, this behavior is dramatically changed. Systems with electrons confined to two-dimensions are realized using semiconductor quantum wells and semiconductor heterostructures. Common candidates of such systems are AlGaAs-GaAs-AlGaAs quantum wells and AlAs-GaAs heterostructures (see e.g. [1, 5–7]). Molecular beam epitaxy (MBE) is used to grow such samples consisting of atomic scale interfaces leading to true two-dimensional electron systems. In 1980, von Klitzing et. al. found that [8] electrons in such a two-dimensional system (metal oxide semiconductor field effect transistor in this case) under high magnetic fields and low temperatures show a quantized Hall resistance (see Fig.1.2).

Under these extreme conditions, the two-dimensional electron gas displays the following unusual behaviors. The main characteristic is the quantization of the Hall resistance. Instead of having a linear dependence with the magnetic field strength, the Hall resistance is found to be showing plateaus at the following values:

$$R_H = \frac{h}{ne^2} \tag{1.2}$$

where h is the Plank constant and e is the electron charge. $n = Be/\rho hc$ takes integer values which are experimentally confirmed now up to the accuracy of seven decimal places. The longitudinal resistance goes to zero (near $T = 0$) in these plateaus. Moreover, the existence

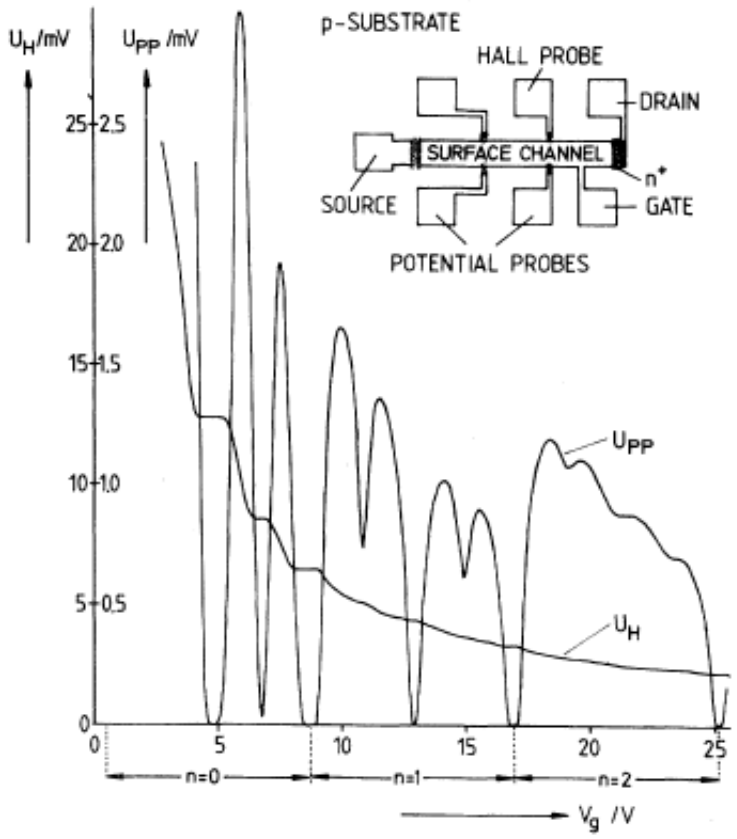

Figure 1.2: Change in Hall voltage U_H and the voltage drop between the recording probes U_{pp} in a constant magnetic field 18 T with respect to the gate voltage V_g. Figure is taken from Ref.[8] with permission.

of plateaus and the corresponding integer values are universal. That is, this behavior is independence of the type of the sample, system size or the geometry. This inherent quantization of the Hall conductance to integer values of e^2/h is called the *Integer Quantum Hall Effect* (IQHE). This effect can be fully explained by quantum mechanics. According to quantum mechanics, when electrons are confined to two-dimensions and subjected to high magnetic fields, their kinetic energy gets quantized into highly degenerate *Landau* levels. IQHE is observed when one or few of these Landau levels are fully occupied by the electrons in the

system. A brief introduction about the formation of Landau levels is given in the subsection below, which will be followed by a theoretical explanation of the IQHE.

1.1.2 Landau Levels

The Hamiltonian for an electron moving in two-dimensional space under a perpendicular magnetic field is given by [9, 10],

$$H = \frac{\vec{\pi}^2}{2m} \tag{1.3}$$

where, m is the non-relativistic effective mass of the electron, and $\vec{\pi}$ is the kinetic momentum expressed in a coordinate representation as follows:

$$\vec{\pi} = -i\hbar\vec{\nabla} + \frac{e\vec{A}}{c} \ . \tag{1.4}$$

Here, $\vec{A}$ is the vector potential such that the perpendicular magnetic field B is given by, $B = \hat{z} \cdot (\vec{\nabla} \times \vec{A})$. It is important to notice that the two kinetic momenta do not commute:

$$[\pi_x, \pi_y] = \frac{i\hbar e}{c}\hat{z} \cdot (\vec{\nabla} \times \vec{A}) = i\frac{e\hbar}{c}B_z = i\frac{\hbar^2}{l_B^2} \ , \tag{1.5}$$

where, l_B is the magnetic length ($l_B^2 = \hbar c/eB$); the length scale of the quantum Hall regime. The magnetic area $2\pi l_B^2$ is equal to one flux quantum h/e leading to the expression, $2\pi l_B^2 B = \Phi_0$.

Now, the Hamiltonian Eq. (1.3) can be solved in the standard manner using ladder

operators,

$$a = \frac{l_B/\hbar}{\sqrt{2}}(\pi_x + i\pi_y) \ , \quad a^\dagger = \frac{l_B/\hbar}{\sqrt{2}}(\pi_x - i\pi_y) \ . \tag{1.6}$$

This formalism gives us the commutation relation,

$$[a, a^\dagger] = 1, \tag{1.7}$$

and the Hamiltonian,

$$H = \hbar\omega\big(a^\dagger a + \frac{1}{2}\big). \tag{1.8}$$

The corresponding Harmonic oscillator energy levels are called the *Landau Levels*. The cyclotron frequency ω is given by $|eB|/mc$. The degeneracy of these Landau levels can be seen by constructing "center of cyclotron motion" operators:

$$X = x + \frac{\pi_y}{m\omega} \ , \tag{1.9}$$

$$Y = y - \frac{\pi_x}{m\omega} \ . \tag{1.10}$$

Notice that, $[X, Y] = -il_B^2$. The x and y coordinates of the cyclotron center do not commute, which is an important property in Landau level physics. Another pair of ladder operators, b and $b^\dagger$ with $[b, b^\dagger] = 1$, can be introduced using these operators:

$$b = \frac{1}{\sqrt{2}l_B}(X - iY) \ , \tag{1.11a}$$

$$b^\dagger = \frac{1}{\sqrt{2}l_B}(X + iY) \ . \tag{1.11b}$$

Moreover, these operators satisfy the following commutation relations.

$$[a, b] = [a^\dagger, b] = [H, b] = 0 \tag{1.12}$$

According to the above commutation relations, the cyclotron-center ladder operator commutes with the one-body kinetic energy operator leading to the production of a degenerate set of energy eigenstates. Therefore, a single-particle Landau level orbital state can be written as follows:

$$|n, m\rangle = \frac{(a^\dagger)^n (b^\dagger)^m}{\sqrt{n!m!}} |0, 0\rangle \ . \tag{1.13}$$

Single-particle wave functions in the lowest Landau level (LLL) can be obtained after choosing a relevant gauge for the vector potential. We choose the symmetric gauge,

$$\vec{A} = \frac{B}{2}(-y, x, 0). \tag{1.14}$$

Using the complex coordinates in the plane, $z = x + iy = re^{i\theta}$ and $\bar{z} = x - iy$, the ladder operators can be written as,

$$b = \frac{1}{\sqrt{2}}\Big(\frac{\bar{z}}{2l_B} + 2l_B\frac{\partial}{\partial z}\Big) \tag{1.15a}$$

$$b^\dagger = \frac{1}{\sqrt{2}}\Big(\frac{z}{2l_B} - 2l_B\frac{\partial}{\partial \bar{z}}\Big) \tag{1.15b}$$

$$a^\dagger = \frac{i}{\sqrt{2}}\Big(\frac{\bar{z}}{2l_B} - 2l_B\frac{\partial}{\partial z}\Big) \tag{1.15c}$$

$$a = \frac{-i}{\sqrt{2}}\Big(\frac{z}{2l_B} + 2l_B\frac{\partial}{\partial \bar{z}}\Big). \tag{1.15d}$$

The vacuum wave function is found by solving $\langle z, \bar{z}|a|0,0\rangle = 0$ and $\langle z, \bar{z}|b|0,0\rangle = 0$. That is, the lowest state in the ladder, $\psi_{0,0}$, should be annihilated by both lowering operators. This gives,

$$\psi_{0,0} = \frac{1}{\sqrt{2\pi l_B^2}} e^{-z\bar{z}/4l_B^2} \ . \tag{1.16}$$

The subsequent application of $b^\dagger$ on the above wave function gives the other degenerate states in the LLL:

$$\psi_{0,m} = \frac{z^m e^{-z\bar{z}/4l_B^2}}{\sqrt{2\pi l_B^2 2^m m!}} \ . \tag{1.17}$$

The z-component of the angular momentum operator is defined as,

$$L_z = -i\hbar\frac{\partial}{\partial\theta} = \hbar(z\frac{\partial}{\partial z} - \bar{z}\frac{\partial}{\partial\bar{z}}) = -\hbar(b^\dagger b - a^\dagger a). \tag{1.18}$$

It is clear that $[H, L_z] = 0$, which implies that the Hamiltonian and the z-component of the angular momentum can be simultaneously diagonalized. The eigenvalue of L_z will be equal to $-m\hbar$. Therefore, the single particle degenerate wave functions in the n^{th} Landau level can be labeled by m $(= -n, -n+1, ..., 0, 1, 2, ...)$.

1.1.3 Planar Geometry

The underlying physics of Landau levels is largely independent of the gauge choice or the geometry in consideration. However, certain gauges in certain geometries turns out to be

the most natural choices to conveniently provide physical descriptions. The symmetric gauge treatment explained above is the most convenient way to see the Landau level physics in the planar geometry because the spherical gauge is manifestly rotationally invariant. The LLL single-particle angular momentum eigenstates are co-centric circles in an infinite plane under symmetric gauge (see Fig.1.3). The radius of such a circle is given by, $r = \sqrt{2m}l_B$, which will depend on the z-component of the angular momentum. Note that this radius does not have any effect on the energy.

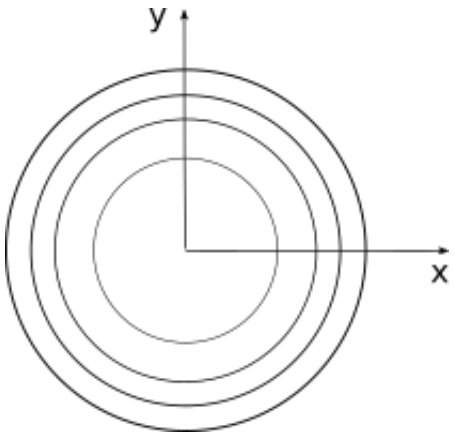

Figure 1.3: Lowest Landau level single-particle states in a disk (symmetric gauge in planar geometry). The radius of a circle is given by, $r = \sqrt{2m}l_B$.

1.1.4 Cylinder Geometry

Another possible choice of gauge is the translationally symmetric gauge. This is also called the Landau gauge.

$$\vec{A} = \frac{B}{2}(-y, 0, 0) \tag{1.19a}$$

$$\vec{A} = \frac{B}{2}(0, x, 0) \tag{1.19b}$$

These gauges preserve the translational symmetry in x or y directions respectively. Let's choose the latter as our gauge to study the LLL structure in a planar strip of width L_y. Moreover, let's implement periodic boundary conditions in the y-direction so that we get the topology of a cylinder. The translational symmetry in the y-direction implies that the single particle wave functions would be plane waves in that direction:

$$\psi(x, y) = \psi(x)\, e^{ik_y y} \ . \tag{1.20}$$

The angular momentum eigenstates labeled by m in the cyliner geometry is infinitely degenerate. The m index goes from negative infinity to the positive infinity. Therefore, instead of "b" operators used in the planar geometry, a unitary magnetic translation operator [11] is relevant in this case, which takes the states labeled by m to other m values. However, the ladder operators "a" are responsible for lowering the LL index. As seen in the symmetric gauge case, the annihilation operators can be expressed in this gauge to be,

$$a = \sqrt{\frac{c}{2e\hbar B}}\frac{\hbar}{i}\Big[\vec{\nabla}_x - \Big(k_y - \frac{eB}{\hbar c}x\Big)\Big] \ . \tag{1.21}$$

In a similar fashion to the symmetric gauge, using these annihilation operators, the LLL single-particle wave functions can be found up to a normalization as the following:

$$\psi(x, y) = exp\Big[ik_y - \frac{eB}{2\hbar c}\Big(x - \frac{\hbar c}{eB}k_y\Big)\Big] \ . \tag{1.22}$$

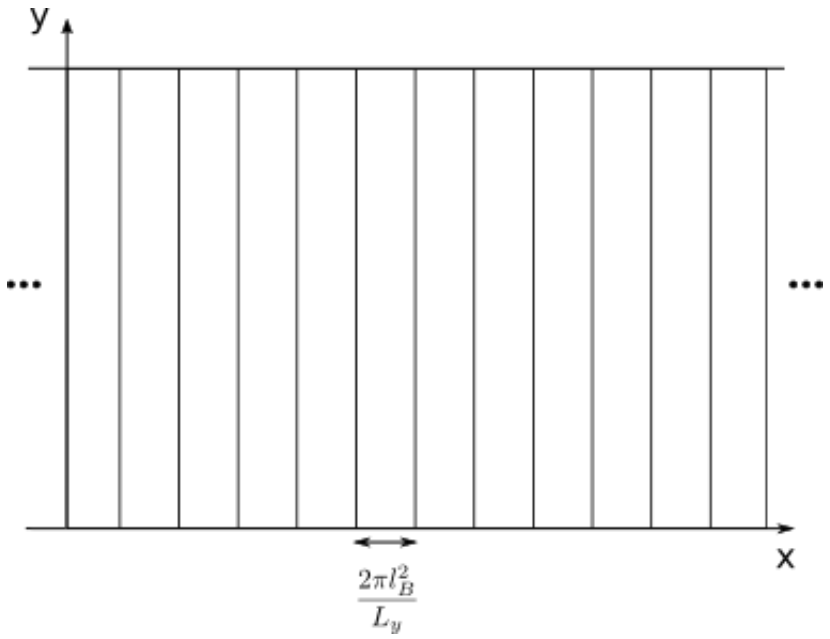

Figure 1.4: Lowest Landau level single-particle states in the cylinder geometry with circumference L_y. Lines depict the highest probability location of the lowest Landau level orbitals. Periodic boundary conditions are implemented in the y-direction. The x positions (guiding centers) are at, $X_m = m\,\kappa\,l_B^2$.

These wave functions are stripes located at $X = k_y l_B^2$; plane waves in y-direction and Gaussian in x-direction. The center of the Gaussian, X depends on $k_y (= 2\pi m/L_y)$ where m is an integer (see Fig.1.4). It is customary to define the inverse radius, $\kappa = 2\pi/L_y$ in the cylinder geometry. The final expression for the single-particle states in the cylinder geometry can be given as (l_B set to 1),

$$\psi_m(z) = \frac{1}{(4\pi^3)^{1/4}} \sqrt{\kappa}\; e^{-\frac{1}{2}(x-m\kappa)^2 + im\kappa y} \;. \tag{1.23}$$

The cylinder geometry is frequently utilized in quantum Hall physics. We have used the cylinder geometry in most of the calculations given in Chapter 2. We express two well known

FQH model Hamiltonians in the cylinder geometry and take an interesting limit of κ going to infinity. Details can be found in Chapter 2.

1.1.5 Spherical Geometry

Spherical geometry is important in the study of quantum Hall states because of the compactness of the sphere, leading to finite dimensional Landau levels. This makes the sphere a preferred geometry to study finite systems. Moreover, the spherical geometry retains full $SU(2)$ rotational symmetry. In order to model a sphere with a radially outward magnetic field, we may theoretically consider a plane wrapped on to the surface of a sphere with a Dirac monopole placed at the center [3, 12, 13]. The total magnetic flux piercing the surface of the sphere can be taken to be $N_\phi \phi_0$, where ϕ_0 being the flux quantum h/e, and N_ϕ being an integer. As mentioned above, the orbital angular momentum (l) and its z-component (m) are good quantum numbers in the spherical geometry. These quantum numbers can assume the following values:

$$l = \frac{N_\phi}{2} \ , \frac{N_\phi}{2} + 1 \ , \frac{N_\phi}{2} + 2 \ , ...$$

$$m = -l \ , -l + 1 \ , ... \ , 0 \ , 1 \ , ... \ , l \ .$$

Landau levels are labeled by the l values starting with $l = \frac{N_\phi}{2}$ for the lowest Landau level. The degenerate single-particle states in the lowest Landau level will be labeled by the corresponding $2l + 1$ values of m. These states are called the *Monopole Harmonics* ($Y_{l,m}$). Therefore, the single-particle states in the lowest Landau level are:

$$Y_{l,m} = \langle r|m\rangle = \Big[\frac{N_\phi + 1}{4\pi}\begin{pmatrix} N_\phi \\ \frac{N_\phi}{2} - m \end{pmatrix}\Big]^{1/2} (-1)^{\frac{N_\phi}{2}-m}\, v^{\frac{N_\phi}{2}-m}\, u^{\frac{N_\phi}{2}+m}\,, \tag{1.25}$$

where,

$$u = cos(\theta/2)\, e^{i\phi/2} \quad \text{and} \quad v = sin(\theta/2)\, e^{-i\phi/2}. \tag{1.26}$$

It is important to note that these single-particle states transform as spin $\frac{N_\phi}{2}$ representation of $SU(2)$. This fact and the other aspects of the quantum Hall physics in the spherical geometry are utilized in some of the calculations explained in Chapter 3.

1.1.6 Theory of the IQHE

The structure of the Landau levels is important in understanding the quantum Hall effects. The IQHE can be fully explained just by Landau level physics [14–18]. A brief qualitative outline of the theory can be given as follows. Breaking of translational symmetry by the presence of disorder is essential to have the IQHE. Some of the single-particle states which were degenerate for the Landau levels in the perfectly clean limit will form localized states in the presence of disorder. This will result Landau levels to be broaden into bands of *extended* and *localized* states. Because of this broadening of Landau levels due to disorder, the energy gaps that were present between two Landau levels in the clean limit are replaced by *mobility gaps* (see Fig.1.5). Only the extended states (which are at the center of the Landau levels) can carry current at zero temperature. In contrast, localized states trap electrons giving no contribution to the current. The effect that disorder causes the appearance of these localized states can be understood semi-classically [16, 17]. The disorder potential can be considered

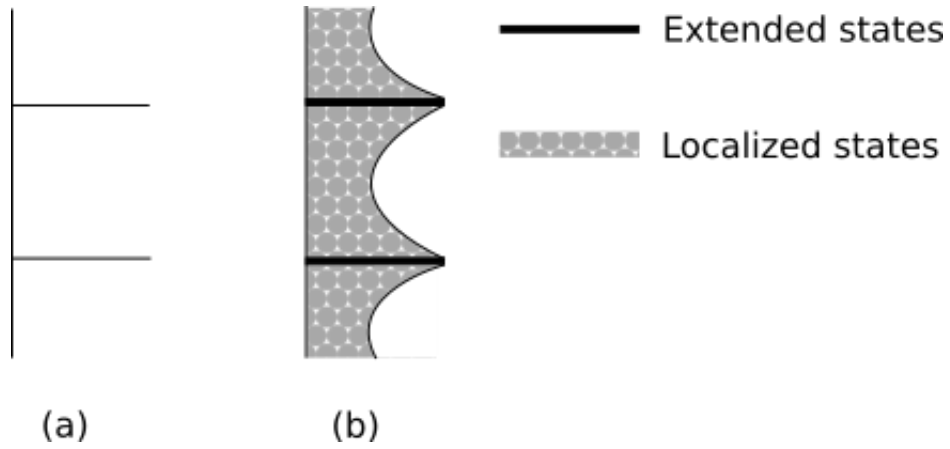

Figure 1.5: (a) Sharp Landau levels in the absence of disorder (b) In the presence of disorder, Landau levels are broadened into bands of extended and localized states.

as smooth potential hills in the sample. Electrons can get trapped in these potential hills resulting in movement along the equipotential lines on the hills. Some of these states will be localized and electrons occupying these states will not contribute to the flow of current. The origin of quantized Hall plateaus can be understood as follows. For simplicity, let's consider that we keep the magnetic field constant and add electrons to the system (rather than changing the magnetic field while keeping the electron density constant, which will have the same effect). Let's assume that the chemical potential of the 2D electron gas is exactly at a Landau level energy. In this case, we first start by filling the extended states. The Hall conductance will increase until all the extended states corresponding to that Landau level have been filled. Then, we start filling the localized states which are in the mobility gap (in between the bands of extended states). These electrons will not contribute to the transport. In this region, the Hall conductance is a constant. When the chemical potential reaches the next band of extended states, the addition of electrons to these states will contribute to

transport resulting in an increase in Hall conductance. Thus we get a plot like Fig.1.2 for IQHE. When n number of Landau levels are filled, there will be n number of plateaus each corresponding to the filling fraction $\nu = n$.

1.1.7 Fractional Quantum Hall Effect

The discovery of IQHE was not the end of the story. In 1982, D.C. Tsui et.al. [19] discovered a plateau in Hall resistance at the filling fraction 1/3. Since then many other plateaus at fractional values have been observed (see Fig.1.6) when high mobility samples and very low temperatures are used in the experiments [20–23]. This effect is called the *Fractional Quantum Hall Effect* (FQHE), the main subject under scrutiny in this thesis.

1.2 Understanding the Fractional Quantum Hall Effect

Given the above understanding of the IQHE, the observation of the FQH effect brought the next experimental surprise which required new theoretical explanations. First of all, the FQH state is a strongly correlated state. With sufficiently large magnetic fields, the Landau level separation is considerably large. Therefore, it is safe to assume that all the electrons in a FQH system occupy only the lowest Landau level (lowest Landau level projection). This leads the kinetic energy to be unimportant in the problem. So, the only important term in the Hamiltonian becomes the electron-electron interaction which is essentially the Coulomb interaction. There are no small parameters in the problem. As a consequence, the non-trivial collective behavior seen in the FQH effect can not be understood as a perturbation to

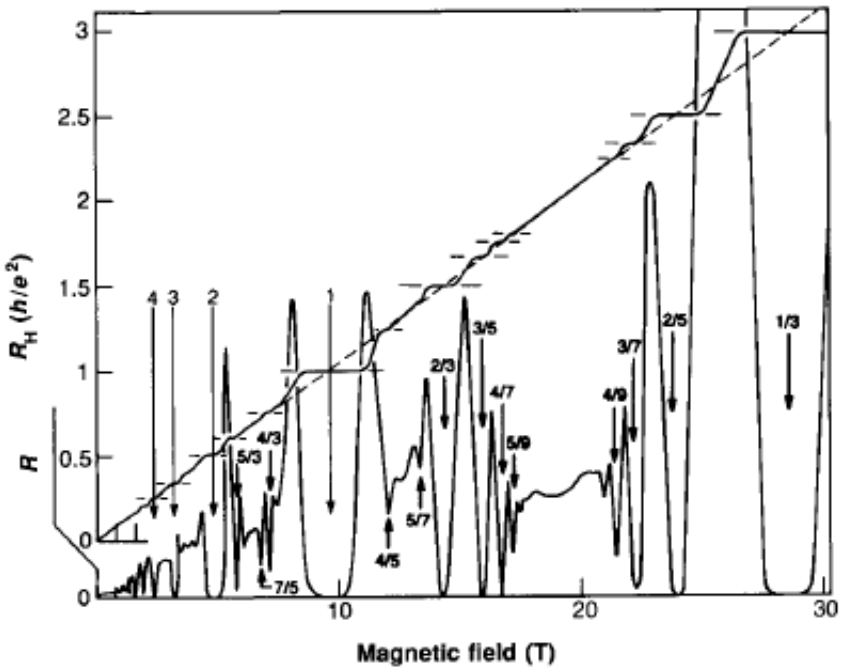

Figure 1.6: Hall resistance R_H and the longitudinal resistance R as a function of magnetic field. The dashed diagonal line represents the classically expected variation. Plateaus of R_H appear in the integer and fractional values corresponding to IQHE and FQHE respectively. R is minimum at the plateaus. Figure is taken from Ref.[24] with permission.

a known solution. Further, it turns out that the FQH effect challenges the Landau-Ginzburg symmetry breaking theory [25, 26], which states that different phases of matter could be identified according to different symmetries in the system. However, FQH systems at various fractions belong to different phases (they can be labeled by different quantum numbers like ground state degeneracy) even though they share the same symmetry. This special kind of phases of matter is called the *Topological Phases of Matter* [27–31]. The existence of fractionally charged quasiparticles [32] is also an inherent property of FQH systems. All of these rather unusual behaviors demand novel theoretical explanations of the FQH effect. In

the following we will briefly discuss some early milestones to this end [2, 3].

1.2.1 Laughlin State

In order to explain the FQHE at the filling fraction 1/3, Laughlin proposed [33] a variational wave function in 1983. This was a many-body wave function for an incompressible quantum fluid. One possible way of obtaining the Laughlin wave function is as follows.

Single-particle wave functions of free electrons in the LLL are given by Eq. (1.17). In strong magnetic fields, the cyclotron energy separation is larger than the interactions. For example, if we consider the $\nu = 1/3$ plateau in Fig. 1.6, which appears around a magnetic field of $30T$, the cyclotron energy separation will be around $600K$ while the Coulomb energy is in the order of $275K$. This suggests that even though the electron-electron interaction energy is smaller than the Landau level separation, it is not smaller by a large factor. Hence Landau level mixing may be an issue in accurate modeling. However, as a starting point, it is still useful to theoretically understand the FQH effect in the infinite magnetic field limit where LLL projection perfectly makes sense. Moreover, it turned out that with some luck this assumption leads to quantitatively acceptable results. Therefore, it is customary to assume that all the electrons are in the LLL. When all the electrons are projected onto the LLL, their kinetic energy is just an unimportant constant. However, in the presence of disorder, as explained in the theory of IQHE, Landau levels get broadened to form bands of extended and localized states. In order to have the FQH effect, the electron-electron interactions should lift the degeneracy and generate an energy gap at fractional filling. Moreover, the

disorder potential should be sufficiently weak. Therefore, much cleaner samples with non-vanishing presence of disorder are needed in this case. Electron-electron interactions play the prominent role in this regime. A Possible many-body state of these strongly correlated electrons could have the following form:

$$\Psi = F_A[z_j]\ exp\Big[-\frac{1}{4}\sum_i |z_i|^2\Big] \tag{1.27}$$

where $F_A[z_j]$ is a polynomial of electron coordinates which is antisymmetric under exchange of those coordinates. Moreover, the structure of the LLL demands $F_A[z_j]$ to be holomorphic. Laughlin observed that he can write down a Jastrow-type variational wave function by assuming the form,

$$F_A[z_j] = \prod_{j<k} f(z_j - z_k)\ . \tag{1.28}$$

Laughlin's choice for such $f(z_j - z_k)$ was $(z_j - z_k)^m$, resulting the full trial wave function for FQHE at $\nu = 1/m$ to be (m- odd integers),

$$\Psi = \prod_{j<k}(z_j - z_k)^m\ exp\Big[-\frac{1}{4}\sum_i |z_i|^2\Big]\ . \tag{1.29}$$

It is remarkable that this trial wave function captures all the important physics of FQH effect at those filling fractions. Moreover, Laughlin's wave function successfully explains the occurrence of fractionally charged quasi-particles in the FQH systems [32]. It turned out that this wave function is the highest density ground state of a model Hamiltonian describing the FQH effect. These are called the Haldane's pseudopotentials, which will be discussed in the

subsection below.

1.2.2 Haldane's Pseudopotential Formalism

The success of Laughlin's remarkable wave function is in part due to its large overlap with states obtained from exact diagonalization of realistic Hamiltonians. In the preceding section, we have already remarked on the importance of LLL projection, both from a purely theoretical point of view as well as making numerical approaches practicable. It was pointed out by Haldane [12] that interactions, specially two-body interactions, are highly constrained by translational and rotational invariance. They are fully parameterized by a discrete set of parameters known as Haldane pseudopotentials, which may often be truncated to a finite set of numbers with acceptable accuracy.

Moreover, it turns out that the V_1 pseudopotential (discussed below) is a model Hamiltonian which exactly stabilizes the Laughlin's 1/3 wave function as its unique highest density ground state. Similar statements can be made for all other ($\nu = 1/m$) Laughlin states. We will briefly describe pseudopotential formalism for two-body interactions in the following. Since the interactions are two-body ($V(z_1 - z_2)$), the Hamiltonian only acts on two-particles at a time. Therefore, as a first step we can decompose the multiparticle wave function into a two-particle wave function times the rest [34]:

$$\Psi(z_1, ..., z_N) = \sum_a \Psi_a(z_1, z_2)\tilde{\Psi}_a(z_3, ..., z_N) \ . \tag{1.30}$$

The two-particle piece of the wave function, $\Psi_a(z_1, z_2)$ can be any two-particle orthogonal

basis at this point. Below, we choose a useful basis for these two-particle wave functions. Since the interaction is isotropic, it only depends on the relative separation of the two particles. Therefore, it is natural to do a center-of-mass and relative decomposition:

$$\Psi(z_i, z_j) = \sum_{b,c} A_{b,c} \Psi_b^{cm}(\frac{z_i + z_j}{2}) \Psi_c^{rel}(z_i - z_j) \ . \tag{1.31}$$

Moreover, we can redefine the ladder operators introduced in subsection 1.1.2, in terms of center-of-mass and relative coordinates $Z \equiv (z_1 + z_2)/2$ and $z \equiv z_1 - z_2$ respectively. Note that the rescaled magnetic lengths $l_R = l_B/\sqrt{2}$ and $l_r = \sqrt{2} l_B$ are being used below. There will be two sets of such ladder operators corresponding to the center-of-mass part and relative part. Only the set of ladder operators for the center-of-mass part is given below:

$$b_R = \frac{1}{\sqrt{2}}\Big(\frac{\bar{Z}}{2l_B} + 2l_B \frac{\partial}{\partial Z}\Big) \tag{1.32}$$

$$b_R^\dagger = \frac{1}{\sqrt{2}}\Big(\frac{Z}{2l_B} - 2l_B \frac{\partial}{\partial \bar{Z}}\Big) \tag{1.33}$$

$$a_R^\dagger = \frac{i}{\sqrt{2}}\Big(\frac{\bar{Z}}{2l_B} - 2l_B \frac{\partial}{\partial Z}\Big) \tag{1.34}$$

$$a_R = \frac{-i}{\sqrt{2}}\Big(\frac{Z}{2l_B} + 2l_B \frac{\partial}{\partial \bar{Z}}\Big). \tag{1.35}$$

Using this decomposition, a complete set of two-particle states in the LLL can be found to be in the following form where M and m are the center-of-mass and relative angular momenta respectively. The operators labeled by "a" are only capable of changing the Landau level index. Therefore, the following LLL states are created just by applying $b_R^\dagger$ and $b_r^\dagger$ on the

vacuum:

$$|M,m\rangle = \frac{(b_R^\dagger)^M (b_r^\dagger)^m}{\sqrt{M!m!}} \,|0,0\rangle \ . \tag{1.36}$$

Note that if particles are fermions (bosons), m must be odd (even). Now, we can insert this complete set of states in the Hamiltonian:

$$\begin{aligned} H &= V(z_i - z_j) \\ &= \sum_{i<j} \sum_{m,m',M,M'} |M',m'\rangle \langle M',m'| \, V(z_i - z_j) \, |M,m\rangle \langle M,m| \ . \end{aligned} \tag{1.37}$$

The Hamiltonian acts only on the relative part. Therefore,

$$\begin{aligned} \langle M',m'| \, V(z_i - z_j) \, |M,m\rangle &= \langle M'|M\rangle \, \langle m'|V(z_i - z_j)|m\rangle \\ &= \delta_{M',M} \, \langle m'|V(z_i - z_j)|m\rangle \ . \end{aligned} \tag{1.38}$$

The rotational invariance of the interaction makes the matrix element diagonal in relative angular momentum quantum number, m:

$$\begin{aligned} H &= \sum_{m,M} |M\rangle \, \langle m'|V(z)|m\rangle \, \langle M| \\ &= \sum_{m,M} V_m \ P_{M,m} \ , \end{aligned} \tag{1.39}$$

where $P_{M,m}$ are projection operators which project onto two-particle states with relative angular momentum m and total angular momentum $M+m$. The coefficients V_m are called the *Haldane pseudopotentials*.

In Section 2.2.2 we will give an application of the Haldane pseudopotential formalism generalized to three-particle interactions. There we will discuss the parent Hamiltonian of the Gaffnian state (a critical phase at $\nu = 2/5$) in both first and second-quantized forms.

Despite Laughlin's nobel-prize-winning breakthrough and the subsequent accomplishments by many other physicists, the quest for complete understanding of the FQH effect still continues at many different levels. There have been numerous trial wave functions proposed to describe the FQH states at various filling fractions. There has been notable progress in understanding the underlying structures of these states such as the matrix product structure [35, 36] and the Jack polynomial structure [37]. The Jack polynomial structure is in many ways related to the thin torus limit [38–41], which is discussed in chapter 2. The effort "dual" to these wave function studies is to find good parent Hamiltonians stablizing these wave functions as their ground states. Studying the low-energy properties of these Hamiltonians has proved to be fruitful because the ground states and the first few excited states capture all the important physics in the FQH regime. In addition, the interesting connections between these microscopic FQH wave functions and the underlying conformal filed theories (CFTs) describing the edge physics have been discovered [42]. Moreover, a correspondence between the bulk and edge physics [43] of the FQH phases has also been established due to the correspondance between underlying CFTs and the topological field theories [44]. The research described in this thesis mainly focuses on studying the low-energy properties of FQH (and more general) Hamiltonians. Nonetheless, these studies make close contact with the corresponding variational wave function based studies and the field theoretic approaches.

The Hamiltonians scrutinized in this thesis are expressed in the second quantized language (see e.g. [45, 46]). Therefore, it would be useful to briefly discuss the second quantization of quantum Hall Hamiltonians and the advantages of using it in FQH regime. In the following section, we briefly introduce the general motivation behind the work reported in this thesis and discuss the second-quantization of quantum Hall Hamiltonians.

1.3 Motivation

The preceding chapters may have provided a rudimentary understanding of the underlying reasons why traditionally, first quantized wave functions and related constructions have been given an unusual preference within the field of FQH physics. This is so especially when compared to other areas of condensed matter physics, from band theory to other branches of strongly correlated physics, where a second quantized formulation is usually preferred as soon as things get technical. Indeed, since the early days, much of the theory of FQH states has been organized around special analytic trial wave functions with very peculiar sets of analytic properties that are only manifest in first quantization. These properties are also instrumental in constructing parent Hamiltonians (see section 2.2.2 below). In turn, these parent Hamiltonians may be used to characterize special trial wave functions as unique smallest angular momentum zero-energy states (zero modes). At higher angular momentum, the zero mode physics of these parent Hamiltonians is very rich, and in many examples leads to recovery of the low-energy effective edge theory of the state in question. As first quantized wave functions, these zero modes share the analytic properties of the incompressible ground state. The study of zero modes of special parent Hamiltonians is therefore a key bridge

between microscopic and effective field theory [1, 12, 37, 47]. This is usually exclusively done in first quantization, although alternatives are recently becoming available [48, 49].

However, the study of zero modes of special parent Hamiltonians certainly does not give access to all spectral features of FQH systems one wishes to understand. Many important properties are buried in finite-energy spectral properties both of special model Hamiltonians (with known zero modes) as well as more generic, realistic Hamiltonians. As is clear from the discussion in sections 1.1.6 and 1.2, the existence of an energy gap to charge excitations in the bulk is a defining feature of quantum Hall systems. Many interesting and topical questions in the field relates to the existence, or not, of such an energy gap, for example in the recently revived debate about the physical nature of the Hall metal state at filling factor 1/2 [50–53]. In addition to that, spectral gap above the ground state is a defining feature of all topological phases (see e.g. [27]). In general, all of the aforementioned nice analytic properties are lost when asking about finite-energy spectral properties of special model Hamiltonians, or when studying realistic models. Therefore, all the advantages of using first quantization are also lost. Therefore, in this thesis we will frequently use the language of second quantization, where a two-body interaction is written in the standard form,

$$H_{int} = \frac{1}{2}\int d^2x d^2x' \Psi^\dagger(x)\Psi^\dagger(x')V(x-x')\Psi(x')\Psi(x) \ , \tag{1.40}$$

where,

$$\Psi(x) = \sum_{r\in\mathbb{Z}} \phi_m(x)^* c_m^\dagger \ . \tag{1.41}$$

Here, the particle creation operator $c_m^\dagger$ creates an electron at the LLL orbital labeled by the angular momentum quantum number, m. As mentioned before we will usually work in the strong field limit where projection onto the LLL is justified. It is worth noting that this projection is not very manifest in the usual first quantized language, which can be criticized for carrying more information than needed, namely information about the dynamical momenta which are really frozen (see e.g. section 1.2), whereas the essential information is carried by the guiding center degrees of freedom [54]. Though often eschewed in the theory of FQH systems, this problem is fully remedied by a formulation in terms of second quantized ladder operators c_m. The latter can be naturally thought of as living on a one-dimensional discrete lattice. Passing to a "guiding center only" language therefore manifestly carries with it a notion of dimensional reduction. In terms of these ladder operators, the typical Hamiltonian will be written as

$$H_{QH} = \sum_{k>0} V_k \sum_R \sum_{x,y} \eta_x^k \, \eta_y^k \, c_{R+x}^\dagger c_{R-x}^\dagger c_{R-y} c_{R+y} \ . \tag{1.42}$$

Here, terms for given k typically correspond to a given Haldane pseudopotential described by form factors η^k in the present formulation. A more careful derivation of such a second quantized Hamiltonian, albeit for a three-body operator, will be given in section 3.2. Conventionally, the general form Eq. (1.42) has been used mostly in numerical work utilizing its manifest dimensional reduction. In this thesis, we will defy this convention and use general second quantized Hamiltonians to make analytic progress on the understanding of low-energy spectral features of FQH systems. Specific questions to be addressed are as follows:

1.4 Outline of the Thesis

The general theme of the work reported in this thesis is to find the low-energy spectral properties of the FQH model Hamiltonians and other general Hamiltonians. The set of energy eigenvalues of a Hamiltonian is called the spectrum of the Hamiltonian. In the proceeding chapters we report studies aimed towards understanding the finite-energy properties of the Hamiltonians often expressed in the second quantized language. Details about the structure of the thesis are given below.

In Chapter 2, we present a "*Thin torus Perturbative Scheme*" to study FQH states. We investigate the Haldane-Rezayi (fermionic) state and Gaffnian (bosonic) state which are at filling fractions $\nu = 1/2$ and $\nu = 2/3$ respectively. Since the underlying conformal field theories are non-unitary for both of these states, they are expected to have gapless excitations in the usual two-dimensional thermodynamic limit. We first construct the two parent Hamiltonians within the framework of second quantization, then by perturbative means study the possible excitations for each case in the thin cylinder/torus limit. We confirm that the gapless excitations are present also in the "one-dimensional" limit for the Haldane-Rezayi state. However, we find that this is not the case for the Gaffnian state and derive an asymptotic expression for the gap. This is confirmed by exploiting numerical direct diagonalization. The thin-torus perturbative scheme developed in this study is a powerful tool. It may be used to extract knowledge about the spectral properties of FQH systems and also other strongly correlated many-body quantum systems. This work has been published in Ref. [55].

Chapter 3 is about the "*Spectral Properties of Positive Many-Body Hamiltonians*". A general class of positive many-body Hamiltonians has been scrutinized in this study. These model Hamiltonians describe the interaction in various systems both in and out of the QH regime where repulsive interactions are involved. We studied these Hamiltonians within the second-quantized framework. We prove a general monotony property of ground state energy with particle number for a general class of Hamiltonians. We find additional constraints for the spectra of positive two-body Hamiltonians with "center-of-mass conserving" symmetry, both in presence and absence of particle-hole symmetry. In particular we constrain the chemical potential at $T = 0$. More importantly, we establish a general bound on the step size of ground state energy with particle number. Subsequently, an upper bound for the charge gap is obtained for systems with zero modes. The results in this study shed light on the evolution of the ground state and the first excited state energies with particle number in previously inaccessible regions. Moreover, the methods developed in this study allow us to obtain the upper bound on the charge gap solely by Hamiltonian properties bypassing the need for the construction of clever variational wave functions. This chapter is based on the Ref. [56].

Chapter 2

THIN TORUS PERTURBATIVE ANALYSISLAVIN OF ELEMENTARY EXCITATIONS IN THE GAFFNIAN AND HALDANE-REZAYI QUANTUM HALL STATES

The ideas of dimensional reduction are of central importance in quantum Hall states. This is rooted in the bulk-edge correspondence for topological phases described by Chern-Simons quantum field theories [44]. This correspondence is also manifest in certain preferred or "special" microscopic trial wave functions used to describe quantum Hall phases, and whose analytic structure is that of conformal blocks of the unitary rational conformal field theory (CFT) describing the edge of the same phase [42]. This situation extends to trial wave functions whose analytic structure is derived from conformal blocks in non-unitary CFTs. Examples of the latter kind are the Gaffnian state [57] and the Haldane-Rezayi [58] state. Here, the physical interpretation of this correspondence is more subtle, as the respective non-unitary CFT is not acceptable as the description of a physical edge. In these cases, it has been argued [57, 59, 60] that a local microscopic Hamiltonian stabilizing such a wave function as ground state must have gapless excitations. In other words, such wave functions are not expected to describe topological (gapped) phases. This conjecture has stimulated numerous theoretical and numerical investigations, [57, 60–66] though providing direct evidence and/or microscopic characterization of the gapless excitations remains an

interesting problem. In the case of the Haldane-Rezayi state, some insight has been obtained by analyzing a thin torus (TT) – or thin cylinder – limit [47]. The TT limit is yet another way to achieve a two-dimensional – one-dimensional (2D–1D) correspondence in the context of quantum Hall systems [38–41, 67–72]. In Ref. [47], the very knowledge of the TT limit of the Haldane-Rezayi (HR) wave-functions was used to argue that charge-neutral gapless excitations must exist in the TT limit, and the latter have been characterized as certain extended equal-amplitude superpositions of defects (see below). In that argument, the detailed form of the HR parent-Hamiltonian was not used, merely the knowledge that it exists and that it has a zero energy ground state. In this chapter, we will show how the features inferred in Ref.[47] can be straightforwardly derived in a perturbative framework, which, as a byproduct, also reveals the proper dependence of the quadratic dispersion on the (thin) cylinder radius. As we will review below, it has been cautioned in Ref. [47] that while the finding of gapless excitations in the thin torus limit is quite plausible evidence for their existence in the 2D thermodynamic limit, the converse is not necessarily true. Indeed, we apply the same perturbative scheme to the Gaffnian state, and find conclusive analytical and numerical evidence that gapless excitations are absent *in the TT limit*. We give an asymptotic formula describing the gap where first the thermodynamic limit is taken in one of two spatial directions and then the TT limit is taken in the other direction. As we discuss in detail in Sec. 2.3, this does not preclude the existence of gapless excitations in the usual 2D thermodynamic limit, though unfortunately, we cannot say more about this from a TT point of view. We hope that nonetheless our investigation will shine interesting light on the

different possible relations between various types of quantum Hall states and their TT limits. Most of the results presented below were published in Ref.[55]. Section 2.2.2 explaining the derivation of the Gaffnian Hamiltonian is added for pedagogical reasons.

2.1 Gapless Excitations in the Haldane-Rezayi state

It has been argued in previous studies [47] that in the TT limit, the gapless character of the Haldane-Rezayi state is manifest in the limiting forms of the associated wave functions. Below we develop a perturbative framework that makes these claims explicit. We focus on the top state in the HR sequence with fermionic filling fraction $\nu = 1/2$.

The two-component HR state is tenfold degenerate [73] on the torus, with eight of ten ground states approaching one of two patterns in the TT limit, up to translations, given in Fig.2.1. Because of the translational symmetry, the two states shown in the figure account

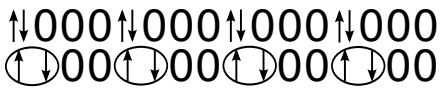

Figure 2.1: Haldane-Rezayi thin torus ground state patterns, in the usual occupation number representation. Zeros denote empty orbitals. The configuration $\uparrow\downarrow$ denotes an up-spin and a down-spin particle occupying the same orbital. Ovals denote spin singlets.

for eight ground states. Note that we refer to the two components of fermions as spin-up and spin-down here and in the following. There are two other special ground states whose TT limits are not fully described by a simple unit cell. These states are in fact closely related to the presence of gapless excitations in HR state. One of these special thin torus HR ground state patterns is given in Fig.2.2, which can be understood as a delocalized singlet immersed

into and separating two ground states of the first kind in Fig.2.1. An explicit calculation using perturbation theory will be given explaining how these excitations acquire zero energy.

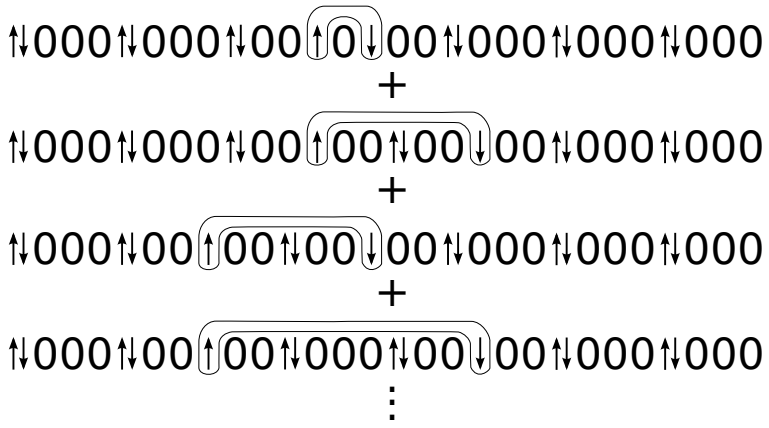

Figure 2.2: The thin torus limit of a particular ground state of the hollow core Hamiltonian. The limiting form is an equal amplitude superposition of states with a delocalized pair of charge-neutral defects forming a singlet.

The HR state is known to be the exact zero energy ground state of the "hollow-core" Hamiltonian [58]. This is just the V_1 Haldane pseudopotential [12], acting between any two electrons regardless of their spin. The name "hollow-core" is alluding to the fact that a V_0-term is allowed between electrons of opposite spin, but is absent in the Hamiltonian. Here we will work mostly on an infinite cylinder with finite circumference $L_y = 2\pi/\kappa$, κ being the inverse radius. A basis for the lowest Landau level in this geometry is naturally given by a set of translationally related orbitals labeled ϕ_r, labeled by an integer r, such that the x-component of the guiding center is well-defined and equal to κr, and we set the magnetic length equal to 1. In second quantized form, the Hamiltonian then takes the form

of a spin-SU(2) invariant two-body operator,

$$H = \frac{1}{2} \sum_{m',n',m,n,\alpha,\beta} V_{m'n'mn}\, C^\dagger_{m',\alpha}\, C^\dagger_{n',\beta}\, C_{n,\beta}\, C_{m,\alpha}\,, \tag{2.1}$$

where C_r destroys a particle in the state ϕ_r, and the matrix element $V_{m'n'mn}$ does not depend on spin indices α, β because of $SU(2)$ invariance. This matrix element is therefore just the same as for the V_1 pseudopotantial in a spin polarized setting, on a cylinder of radius $1/\kappa$, which is standard in the literature (see, e.g., Ref. [74]). This gives (with arbitrary but κ-independent overall normalization):

$$\begin{aligned} H &= \sum_R \sum_{\alpha,\beta} \sum_{\substack{m'+n'=2R \\ m+n=2R}} \kappa^3 (m-n)(m'-n') \\ &\times \quad e^{-\kappa^2[(m-n)^2+(m'-n')^2]/4}\, C^\dagger_{m',\alpha}\, C^\dagger_{n',\beta}\, C_{n,\beta}\, C_{m,\alpha} \end{aligned} \tag{2.2}$$

Now that spin-1/2 degrees of freedom are present in the problem, it should be noted that the pair-interaction defined by Eq. (2.2) still only acts on triplet pairs. This is natural, since in the infinite plane, the V_1-pseudopotential is defined as a two-particle projection operator projecting on states with relative orbital angular momentum 1. No pair forming a spin singlet can have this relative angular momentum. On the cylinder/torus geometry, however, relative angular momentum is not well-defined. Hence it is worth noting that the fact remains that the interaction annihilates any singlet pair. This follows already from the fact that the matrix element $V_{m'n'mn}$ is anti-symmetric in m and n (as well as their primed counterparts) whereas any two-particle singlet state must have a symmetric orbital part.

We now use the second-quantized Hamiltonian (2.2) to set up a perturbative scheme designed to calculate energies and states in powers of $x = e^{-\frac{1}{2}\kappa^2}$. To this end we write the Hamiltonian as

$$H = H_0 + \lambda H_1 \,, \tag{2.3}$$

where $\lambda = 1$ is a formal parameter. H_0 contains all terms in the Hamiltonian (2.2) that are diagonal in the *orbital* indices. That is, all terms for which the unordered pairs (m, n) and (m', n') are equal, whereas spin indices may or may not be equal. H_1 contains all the remaining, off-diagonal terms. We will perform a double expansion. The first of these is the formal expansion in the parameter λ. It turns out that each order in λ receives multiple contributions (infinitely many, for infinite system size) in the different powers of the parameter x. At any fixed order in λ, we will therefore retain only those orders of x that we are interested in. We claim that in this way, to get all contributions of a certain order x^ℓ exactly, one needs to go only to a certain finite order in λ, which will depend on ℓ. We will not attempt a formal proof of this statement, but it will become quite apparent that for higher and higher orders in λ, the leading order in x will grow systematically. In our case, we will be interested in terms up to 12th order in x, for which second order perturbation theory in λ will be sufficient.

We will first focus on the odd particle number sector, for which one has two degenerate ground state doublets on the torus [75]. The relevant thin torus states are discussed in Ref.[47]. They are obtained as a superposition of states of the form shown in Fig.2.3, where a single spin-1/2 defect becomes delocalized in a ground state pattern of the A-type (the

first of the ground state patterns in Fig. 2.1).

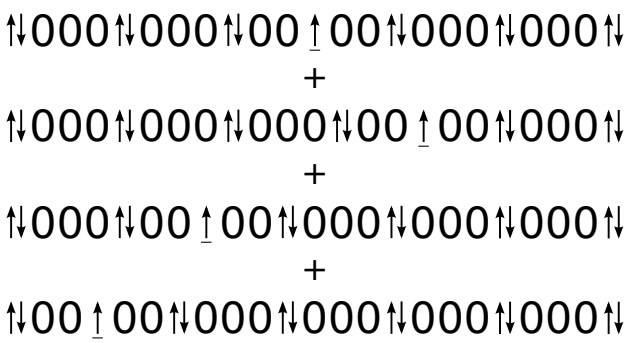

Figure 2.3: A spin-1/2 deffect becomes delocalized in an A-type ground state pattern

Clearly, all states contributing to this superposition are degenerate for H_0, and hence we must apply degenerate perturbation theory in λ. The leading non-trivial order in x turns out to be x^{12}, and we shall be content with this order. For this, it turns out to go to second order in λ. Order-λ^0 diagonal matrix elements are dominated by the interaction of the spin-1/2 defect with two neighboring singlets at distance 3. It is easy to see from Eq. (2.2) that each "bond" between a spin-1/2 defect and one such neighboring singlet costs an energy of

$$E_0 = 54x^9 \,. \tag{2.4}$$

We shall now consider corrections up to order x^{12} arising in second order degenerate perturbation theory in λ. For simplicity, we will first consider a three particle system. The two (H_0–)degenerate thin cylinder ground states are:

$$|\Omega_1\rangle = C^\dagger_{0,\uparrow} C^\dagger_{3,\downarrow} C^\dagger_{3,\uparrow} \tag{2.5}$$

$$|\Omega_2\rangle = C^\dagger_{1,\downarrow} C^\dagger_{1,\uparrow} C^\dagger_{4,\uparrow} \, . \tag{2.6}$$

We also truncate the Hilbert space to consist of five orbitals $r = 0 \ldots 5$, limiting ourselves to the following two excited states:

$$|\Psi_1\rangle = \frac{1}{\sqrt{2}} (C^\dagger_{1,\uparrow} C^\dagger_{2,\uparrow} C^\dagger_{3,\downarrow} - C^\dagger_{1,\downarrow} C^\dagger_{2,\uparrow} C^\dagger_{3,\uparrow}) \tag{2.7}$$

$$|\Psi_2\rangle = \frac{1}{\sqrt{6}} (C^\dagger_{1,\uparrow} C^\dagger_{2,\uparrow} C^\dagger_{3,\downarrow} - 2C^\dagger_{1,\uparrow} C^\dagger_{2,\downarrow} C^\dagger_{3,\uparrow} + C^\dagger_{1,\downarrow} C^\dagger_{2,\uparrow} C^\dagger_{3,\uparrow}) \tag{2.8}$$

Using spin-rotational and other symmetries, these are the only two states in the truncated Hilbert space that our unperturbed states can mix with. Note that they are both H_0-eigenstates, though not of the same energy, having energies $6x$ and $2x + 96x^4$ respectively, owing to spin fluctuations that are kept in H_0. In second order degenerate perturbation theory, one then has the following correction to the diagonal matrix element:

$$\begin{aligned} E^{(2)}_{diag} &= \frac{|\langle \Psi_1 | H_1 | \Omega_1 \rangle|^2}{0 - E^{(0)}_{\Psi_1}} + \frac{|\langle \Psi_2 | H_1 | \Omega_1 \rangle|^2}{0 - E^{(0)}_{\Psi_2}} \\ &= -54\, x^9 + 1296\, x^{12} - \mathcal{O}(x^{15}) \, , \end{aligned} \tag{2.9}$$

where we have only kept terms up to order x^{12}. This reduces these diagonal matrix elements

to an energy of order x^{12}, which we denote by V:

$$V = E_0 + E^{(2)}_{diag} \tag{2.10}$$

$$V = 1296\, x^{12} - \mathcal{O}(x^{15})\,. \tag{2.11}$$

Similarly, the off-diagonal matrix element is obtained as

$$\begin{aligned} -t &= E^{(2)}_{off-diag} \\ &= \frac{\langle\Omega_2|H_1|\Psi_1\rangle\,\langle\Psi_1|H_1|\Omega_1\rangle}{0 - E^{(0)}_{\Psi_1}} + \frac{\langle\Omega_2|H_1|\Psi_2\rangle\,\langle\Psi_2|H_1|\Omega_1\rangle}{0 - E^{(0)}_{\Psi_2}} \\ &= -1296\, x^{12} + \mathcal{O}(x^{15}). \end{aligned} \tag{2.12}$$

At order x^{12}, we thus have $t = V$, as was correctly inferred from less direct arguments in Ref. [47]. At order x^{12}, we thus obtain the effective Hamiltonian

$$H_{eff} = \begin{pmatrix} V & -V \\ -V & V \end{pmatrix}, \tag{2.13}$$

leading to a single zero energy eingenstate, which is the equal amplitude superposition of $|\Omega_1\rangle$ and $|\Omega_2\rangle$, as expected. The energy of the other member of the formerly degenerate pair is $E_{ext} = 2V$.

One may ask if our perturbative scheme is valid, since both zeroth order and second order matrix elements in λ were of the same order x^9 in x. At least for the 3-particle problem, this question can be settled exactly. The full Hamiltonian in this truncated Hilbert space

corresponds to the 4x4 matrix

$$\begin{pmatrix} 54x^9 & -\frac{18}{\sqrt{2}}x^5 & -\frac{18}{\sqrt{6}}x^5 & 0 \\ -\frac{18}{\sqrt{2}}x^5 & 6x & 0 & -\frac{18}{\sqrt{2}}x^5 \\ -\frac{18}{\sqrt{6}}x^5 & 0 & 2x+96x^4 & \frac{18}{\sqrt{6}}x^5 \\ 0 & -\frac{18}{\sqrt{2}}x^5 & \frac{18}{\sqrt{6}}x^5 & 54x^9 \end{pmatrix}.$$

It can be shown exactly that this matrix has one lowest eigenvalue at zero, with the next higher up eigenvalue being

$$\begin{aligned} E_{ext} &= x + 48x^4 + 27x^9 \\ &- x\sqrt{1+3x^3(32+768x^3+18x^5-864x^8+243x^{13})} \end{aligned} \tag{2.14}$$

Expanding the above up to order x^{12}, one finds $E_{ext} = 2V$ in agreement with our perturbative approach. Higher orders in λ will thus only contribute subdominant terms in x.

Turning to the N-particle problem defined by the Hamiltonian (2.3) and the H_0-degenerate subspace described in figure 2.3, we have, first of all, contributions to the effective Hamiltonian H_{eff} that are exactly analogous to those in the 3-particle problem discussed first. We still find no other processes, at second or higher oder in λ, that contribute to order x^{12} or less in x. Therefore, the picture is similar to the 3-particle problem. At order x^{12}, each state in Fig. 2.3 has a diagonal energy of $2V$ (V for each neighboring singlet of the defect). On

top of that, we have a hopping matrix element of the form shown in Fig. 2.4, with $t = V$.

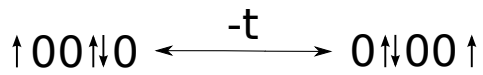

Figure 2.4: The off-diagonal matrix element delocalizing spin-1/2 defects.

The defect thus acquires a gapless quadratic dispersion of the form

$$E(k) = 2V - 2V\cos(k)\,, \tag{2.15}$$

as predicted in Ref. [47] with $V = 1296\,x^{12} + \mathcal{O}(x^{13})$. The state corresponding to $k = 0$ is the zero energy ground state corresponding, in the TT limit, to the equal amplitude superposition of the states shown in Fig. 2.3.

Next we discuss the case of even particle number. In this case, the relevant H_0-degenerate subspace is given by all states of the form indicated in Fig. 2.2. Diagonal energies are now of the form $4V$ (except for states such as the first shown in the figure, see below), and we still have the effective defect-hopping shown in Fig. 2.4, with $t = V$. It is found that the equal amplitude superposition of Fig. 2.2 still gives a zero energy state. The only additional subtlety arises from configurations where the two defects are in closest proximity, as the first shown in the figure. It was conjectured in Ref. [47] that there should be no energy associated with the two neighboring defects, as long as the latter are forming a singlet. We have already discussed above why this is indeed the case, as the Hamiltonian only acts on triplet pairs. The diagonal energy of such configurations is thus $2V$, and this is exactly

required to satisfy the "detailed balance" condition giving a zero energy state. Moreover, it is clear on variational grounds that boosting the momentum of the delocalized pair would give rise to orthogonal states of arbitrarily small energy, in the thermodynamic limit. Indeed, using the matrix elements discussed here, it is easy to generalize Eq. (2.15) to the problem of two defects of "rapidities", k_1 and k_2, respectively, for which there will be an eigenstate of energy $E(k_1) + E(k_2)$, with $E(k)$ as given by Eq. (2.15).

We have thus verified all of the conjectures made in Ref. [47], going up to orders x^{12} in a perturbative framework. At higher order in x, we expect that while corrections will be non-trivial, the observed "detailed balance" between diagonal and off-diagonal terms observed at the present order will continue to hold and lead to the presence of a zero mode. This must, of course, be true from the fact that first quantized zero mode wave functions can be given exactly that do have delocalized defects of the form presented here in the TT limit. The arguments for gapless excitations given in Ref. [47], which we have verified explicitly at the lowest non-trivial order in perturbation theory here, are expected to hold to all orders. For self-containedness, we briefly repeat and sharpen these arguments in the following. First of all, in the sector that has only a single defect, one would still find a tight-binding type dispersion for this defect, with longer ranged but exponentially decaying hopping terms. This dispersion must have its bottom edge precisely at zero to any order in perturbation theory, as we explained above. Hence, for the single-defect sector (which requires particle number to be odd), the gapless character of the TT limit follows.

In the even particle number case, there must be two defects, which, at higher orders in

perturbation theory, may interact in more complicated ways than found at the present order. We do know, however, that despite this interaction, there will be a zero mode to all orders in perturbation theory, featuring two delocalized defects forming a singlet. Again, this is known since the wave functions having this behavior can be given exactly. Moreover, the interaction between these defects will be exponentially decaying. For these two degrees of freedom in an infinite system, general results in scattering theory [76] imply that such local interactions do not change the absolutely continuous spectrum of the theory. If we adiabatically switch off the interactions, we are back to the spectrum associated to two single defects, which is continuous and has its bottom edge at zero, as discussed above. Hence this is also true in the presence of the interaction. Moreover, we know that the interaction cannot cause any bound states to appear below zero energy, since the Hamiltonian is known to be positive. Thus, the observation that the spectrum has a continuum above its lowest value at zero for the sector containing two delocalized singlet defects must continue to hold at any order in perturbation theory. The only difference at the order given here is that the corresponding eigenstates can be worked out easily from the given matrix elements.

2.2 Thin torus elementary excitations in the Gaffnian state.

2.2.1 General considerations

The Gaffnian wave function is a state of particles at filling factor $\nu = 2/3(2/5)$ for bosons(fermions) [57]. Its parent Hamiltonian is a three-particle interaction, and has been extensively discussed [57, 77]. We will focus on the bosonic case here for simplicity. On the torus, the ground state is 6-fold degenerate, with thin torus states approaching the patterns $200200200\ldots$,

110110110..., including translations. We wish to investigate if a scenario similar to that of the HR state is realized, and gapless excitations can be identified in the TT limit.

One main difference between the Gaffnian and HR case is the fact that none of the Gaffnian ground states look "suspicious" in the TT limit, whereas the HR state has ground states (among others) whose TT limit is the equal amplitude superposition shown in Fig. 2.2. From the latter, all features derived in the preceding section have been correctly inferred previously [47]. Here we investigate a scenario that could nonetheless explain the existence of Gaffnian gapless excitations of a similar flavor to those discussed for the HR. Unfortunately, we find that details of this scenario do not work out, and the excitations we discuss are gapped in the TT limit. However, from comparison with numerics, we do find that these excitations are indeed the lowest energy excitations in the TT limit, and hence the TT limit of the Gaffnian state is gapped.

A class of parent Hamiltonians for the Gaffnian state can be written as [57]

$$H = V_0 P_3^0 + V_2 P_3^2 , \tag{2.16}$$

where V_0 and V_2 are positive constants, and P_3^0 and P_3^2 are 3-particle projection operators that project onto the subspace of relative angular momentum 0 and 2, respectively. Using the results of Ref. [78] (for pedagogical reasons this result will be proved in the following subsection), this interaction is readily presented in second quantized form:

$$H = \sum_R \left(q_R^\dagger\, q_R + C\, Q_R^\dagger Q_R\right)$$

Where,

$$\begin{aligned} Q_R = & \sum_{\substack{m+n+l= \\ 3R}} \left\{1 - \kappa^2\Big[(R-m)^2 + (R-n)^2 + (R-l)^2\Big]\right\} \\ & \times e^{-\kappa^2\left[\frac{(R-m)^2+(R-n)^2+(R-l)^2}{2}\right]} C_n C_m C_l \\ q_R = & \sum_{\substack{m+n+l= \\ 3R}} e^{-\kappa^2\left[\frac{(R-m)^2+(R-n)^2+(R-l)^2}{2}\right]} C_n C_m C_l\,, \end{aligned} \tag{2.17}$$

where $C > 0$ is a constant that controls the relative strength between the two terms in Eq. (2.16), and we have chosen an overall normalization.[1] In Eq. (2.17), the summation over R is over all values such that $3R$ is an integer. A detailed calculation of this result is given below.

2.2.2 Gaffnian Hamiltonian

Well-known fractional quantum Hall states like Laughlin states, the Moore-Read Pfaffian, Haffnian and Read-Rezayi parafermion states [33, 42, 79, 80] can be identified as the unique lowest-degree symmetric analytic functions that vanish as a certain power p when some $(g+1)$ number of particles are brought together. This is also known as the clustering condition [81]. Moreover, these functions are the exact highest density zero energy states of some model

[1]Here, we omit an overall factor κ^2, that is also not present in Ref. [78]. It needs to be included if a κ-independent normalization of pseudopotentials is desired, but is of no consequence in the present context.

Hamiltonians constructed from $(g+1)$ particle projection operators [77].

Let's denote the relative angular momentum of $(g+1)$ particles by L_{g+1}. The minimum of the relative angular momentum will be,

$$L_{g+1}^{min} = \begin{cases} \dfrac{g(g+1)}{2} & \text{for Fermions} \\ 0 & \text{for Bosons.} \end{cases}$$

In constructing the model Hamiltonians, a corresponding $(g+1)$ particle angular momentum projection operator can be considered that projects onto any state where a cluster of $(g+1)$ particles has a relative angular momentum $L_{g+1} < L_{g+1}^{min} + p$. Using this notation we can identify the corresponding values for g and p for some of the common FQH states as given in Table (2.1).

Notation		
g	p	Name of the State
1	any p	Lauglin
any g	1 and 2	Read Rezayi
2	4	Haffnian
2	3	Gaffnian
2	2	Pfaffian

Table 2.1: The Number of particles in a cluster $(g+1)$, and the angular momentum projection, $L_{g+1} < L_{g+1}^{min} + p$ for different quantum Hall states.

According to the above formalism, a Gaffnian parent Hamiltonian that stabilizes the Gaffnian wave function as its ground state can be constructed as follows [57]. The Gaffnian wave function is the unique lowest degree, symmetric, analytic wave function that vanishes as at least $p = 2$ powers when three particles are brought together. The model Hamiltonian

is therefore given by the sum of projection operators for all possible $(g+1)$ particle clusters, where each projection operator projects onto the subspace of bosonic (fermionic) state with relative angular momentum $L = 0$ *or* $L = 2$ ($L = 3$ *or* $L = 5$). Here, we will explicitly construct the second quantized form of this Hamiltonian.

To this end, we will first construct an explicit first quantized form of this interaction. We start with the following ansartz (which we are not aware of having been explicitly discussed in the literature before):

$$H = (\nabla_1^4 + \nabla_2^4 + \nabla_3^4)\, \delta(z_1 - z_2)\delta(z_1 - z_3) \tag{2.18a}$$

where,

$$\nabla_i^2 = 4\, \partial_{z_i} \partial_{z_i^*} \quad ; i = 1, 2, 3 \ . \tag{2.18b}$$

As usual, z_i denotes the position coordinates of the i^{th} particle on a plane ($z = x + iy$). It is clear that the above equation is a three-body interaction. Therefore, it is necessary to generalize the Haldane's original two-body pseudopotential formalism [12] as discussed in section 1.2.2 to 3-body interactions [34]. Since the Gaffnian Hamiltonian will act on three particles at a time, we can decompose the general N-particle wave function in the following way and focus only on the 3-particle part. Note that the three-body part of the wave function can be any basis at this point:

$$\psi(z_1, ..., z_N) = \sum_a \psi_a(z_1, z_2, z_3)\tilde{\psi}_a(z_4, ..., z_N) \ . \tag{2.19}$$

The 3-body wave function can be further decomposed in to center of mass and relative parts. The Hamiltonian which is translationally invariant (which only depends on the relative coordinates) will act only on the relative part of the wave function. Considering the structure of the single-particle wave functions of the Landau level orbitals in a planar geometry, where the relative part of the wave function is made of a polynomial times a Gaussian factor, we write the following.

$$\begin{aligned}\psi_(z_1,z_2,z_3) &= \sum_{b,c} A_{b,c}\ \psi_b^{CM}(\frac{z_1+z_2+z_3}{3})\ \tilde{\psi}_c^{rel}(z_1,z_2,z_3) \\ &= \sum_{b,c} A_{b,c}\ \psi_b^{CM}(\frac{z_1+z_2+z_3}{3})\ \psi_c^{rel}(z_1,z_2,z_3)\, e^{[-\frac{1}{4}(|z_1|^2+|z_2|^2+|z_3|^2)]} \end{aligned} \quad (2.20)$$

The relative angular momentum L is a good quantum number to label the complete set of states ψ^{rel}. The rotational symmetry of the interactions makes the matrix elements diagonal in L.

$$\psi(z_1,z_2,z_3) = \sum_L A_L\ \psi_L^{CM}(\frac{z_1+z_2+z_3}{3})\ \psi_L^{rel}(z_1,z_2,z_3)\, e^{[-\frac{1}{4}(|z_1|^2+|z_2|^2+|z_3|^2)]} \quad (2.21)$$

For technical reasons, we can further use a change of variables, $w_1 = z_1 - z_2$, $w_2 = z_1 - z_3$, $W = \frac{z_1+z_2+z_3}{3}$ and their complex conjugates to get the following general form of the wave function:

$$\begin{aligned}\psi(w_1,w_2,W,w_1^*,w_2^*,W^*) &= \sum_L A_L\, \psi_L(W,W^*)^{CM}\, \psi_L(w_1,w_2,w_1^*,w_2^*)^{rel} \\ &\times\ e^{[-\frac{1}{4}(3|W|^2+\frac{2|w_1|^2+2|w_2|^2-w_1^*w_2-w_1w_2^*}{3})]}\ . \end{aligned} \quad (2.22)$$

To find the relative part of the (bosonic) wave function, we use the *symmetric polynomials*, $e_{m,n}(\tilde{z_1}, \tilde{z_2}, \tilde{z_3})$. First two of these will be

$$\begin{aligned} |L=0\rangle &= 1 \\ |L=2\rangle &= e_{2,3}(\tilde{z_1}, \tilde{z_2}, \tilde{z_3}) = \tilde{z_1}\tilde{z_2} + \tilde{z_1}\tilde{z_3} + \tilde{z_2}\tilde{z_3} = \frac{1}{3}(-w_1^2 + w_1 w_2 - w_2^2) \ , \end{aligned} \tag{2.23}$$

where,

$$\begin{aligned} \tilde{z_1} &= z_1 - \frac{1}{3}(z_1 + z_2 + z_3) &= \frac{1}{3}(w_1 + w_2) \\ \tilde{z_2} &= \frac{1}{3}(2 + z_2 - z_1 - z_3) &= \frac{1}{3}(-2w_1 + w_2) \\ \tilde{z_3} &= \frac{1}{3}(2 + z_3 - z_1 - z_2) &= \frac{1}{3}(w_1 - 2w_2) \ . \end{aligned} \tag{2.24}$$

The eigenfunction labeled by the relative angular momentum 3, $|L=3\rangle$ will have the degree-3 terms and eventually contribute zero upon calculating the matrix elements of the local Hamiltonian as shown below(In the delta function integration we put all w_i and w_i^* to zero on the boundary). The matrix elements of the local Hamiltonian can be calculated using the fact that the center of mass part of the wave function will be orthogonal to each other.

$$\begin{aligned} \langle\psi|(\nabla_1^4 + \nabla_2^4 + \nabla_3^4)\,\delta(z_1 - z_2)\delta(z_1 - z_3)|\phi\rangle &= \tfrac{12}{9} \int dW\, dW^*\, \tilde{\psi}_0^{CM} \phi_0^{CM} e^{(-\frac{3}{2}|W|^2)} \\ &\quad + \tfrac{24}{9} \int dW\, dW^*\, \tilde{\psi}_2^{CM} \phi_2^{CM} e^{(-\frac{3}{2}|W|^2)} \end{aligned} \tag{2.25}$$

It is also trivial to calculate the matrix elements for a Moore-Read like local Hamiltonian as

the following.

$$\langle\psi|\delta(z_1-z_2)\delta(z_1-z_3)|\phi\rangle = \frac{1}{8}\int dW\, dW^*\, \tilde{\psi}_0^{CM}\phi_0^{CM} exp(-\frac{3}{2}|W|^2) \tag{2.26}$$

Now, from the definition of the Gaffnian Hamiltonian, we know that it should project out all the states with relative angular momentum less than or equal to two ($L<3$). Therefore, the corresponding matrix elements (see Eq. (2.16)) would be

$$\begin{aligned}
\langle\psi|P_3^2|\phi\rangle &= \Big(\sum_L \psi_L^{CM}(\frac{z_1+z_2+z_3}{3})\,\psi_L^{rel}(z_1,z_2,z_3)\,e^{[-\frac{1}{4}(|z_1|^2+|z_2|^2+|z_3|^2)]}\Big) \\
&\times\ P_3^3\Big(\sum_L \psi_L^{CM}(\frac{z_1+z_2+z_3}{3})\,\psi_L^{rel}(z_1,z_2,z_3)\,e^{[-\frac{1}{4}(|z_1|^2+|z_2|^2+|z_3|^2)]}\Big) \\
&= \frac{1}{8}\int dW\, dW^*\, \tilde{\psi}_0^{CM}\phi_0^{CM} e^{(-\frac{3}{2}|W|^2)}\int dw_1\, dw_1^* dw_2\, dw_2^* \\
&\times\ e^{(-\frac{1}{2}\frac{2|w_1|^2+2|w_2|^2-w_1^*w_2-w_1w_2^*}{3})} + \frac{1}{8}\int dW\, dW^*\, \tilde{\psi}_2^{CM}\phi_2^{CM} e^{(-\frac{3}{2}|W|^2)} \\
&\times\ \int dw_1\, dw_1^* dw_2\, dw_2^*\, \frac{1}{9}\Big(-(w_1^*)^2+w_1^*w_2^*-(w_2^*)^2\Big) \\
&\times\ \Big(-w_1^2+w_1w_2-(w_2)^2\Big) e^{(-\frac{1}{2}\frac{2|w_1|^2+2|w_2|^2-w_1^*w_2-w_1w_2^*}{3})} \\
&\times\ e^{(-\frac{1}{2}\frac{2|w_1|^2+2|w_2|^2-w_1^*w_2-w_1w_2^*}{3})}\ .
\end{aligned} \tag{2.27a}$$

The Gaussian integrals in the above expression can be calculated using the Wick's Theorem [82] to get

$$\begin{aligned}
\langle\psi|P_3^2|\phi\rangle &= 6\pi^2\int dW\, dW^*\, \tilde{\psi}_0^{CM}\phi_0^{CM} e^{(-\frac{3}{2}|W|^2)} \\
&+\ 24\pi^2\int dW\, dW^*\, \tilde{\psi}_2^{CM}\phi_2^{CM} e^{(-\frac{3}{2}|W|^2)}\ .
\end{aligned} \tag{2.27b}$$

Similarly the matrix element for the projection operator P_3^0 will be

$$\langle\psi|P_3^0|\phi\rangle = 6\pi^2 \int dW\, dW^*\, \tilde{\psi}_0^{CM} \phi_0^{CM} e^{(-\frac{3}{2}|W|^2)} \ . \tag{2.28}$$

In the above expressions we have expressed the P_3^2 and P_3^0 projection operators and their local forms Eq. (2.25) and Eq. (2.26) in terms of the center of mass wave functions. Now we can eliminate the center of mass wave functions and express the above projection Hamiltonians in terms of the local forms. After that, we can use the LLL single-particle wave functions on the cylinder geometry to calculate the second quantized form of the Gaffnian Hamiltonian as shown below.

We consider the 2D system to be projected on to a quasi-1D lattice where each orbital is denoted by the angular momentum quantum number. Let's consider the general case where three particles in the orbitals m, n and l hop to m', n' and l' orbitals in such a way that they conserve the center of mass coordinate:

$$P_3^2 \ = \ \frac{1}{6} \sum_{m,n,l} \sum_{m',n',l'} V^{(2)}_{m'n'l'mnl}\, C^\dagger_{m'}\, C^\dagger_{n'}\, C^\dagger_{l'}\, C_l\, C_n\, C_m \ , \tag{2.29a}$$

where,

$$\begin{aligned} V^{(2)}_{m'n'l'mnl} \ &= \ \mathcal{S}_{(m'n'l')(mnl)} \int dz_1\, dz_1^* dz_2\, dz_2^*\, dz_3\, dz_3^*\, \psi^*_{m'(z_1)}\, \psi^*_{n'(z_2)}\, \psi^*_{l'(z_3)} \\ &\times \ \{(\nabla_1^4 + \nabla_2^4 + \nabla_3^4)\, \delta(z_1 - z_2)\delta(z_1 - z_3)\}\, \psi_{m(z_1)}\, \psi_{n(z_2)}\, \psi_{l(z_3)} \ . \end{aligned} \tag{2.29b}$$

Here, $\mathcal{S}_{(m'n'l')(mnl)}$ denotes symmetrization over the given indices. Moreover, as discussed in Chapter 1, the LLL single-particle wave functions on the cylinder geometry are (κ-dependent normalization is omitted),

$$\begin{aligned} \psi_{n(z)} &= \xi^n \, exp(-\frac{1}{2}(x^2 + \kappa^2 n^2)) && \text{(2.30a)} \\ \kappa &= \frac{2\pi}{L_y} && \text{(2.30b)} \\ \xi &= e^{\kappa z} \ . && \text{(2.30c)} \end{aligned}$$

In order to perform the integral in Eq. (2.29b), we can use the following change of variables:

$$\begin{aligned} p = m - n \qquad & r = m' - n' \\ q = m - l \qquad & s = m' - l' \\ t = n - l \qquad & u = n' - l' \end{aligned}$$

$$R = \frac{m+n+l}{3} = \frac{m'+n'+l'}{3} \ . \tag{2.31}$$

After integration we do the symmetrization to get the following matrix element, now expressed in terms of the relative angular momentum coordinates:

$$\begin{aligned} V^{(2)}_{m'n'l'mnl} &= \frac{2 \times 4^3}{8 \times 81}\sqrt{\frac{\pi}{3}}\{\kappa^4(p^2 - pq + q^2 - \frac{3}{2\kappa^2})(r^2 - rs + s^2 - \frac{3}{2\kappa^2})\} \\ &\times \ e^{-\frac{1}{3}(p^2 - pq + q^2 + r^2 - rs + s^2)} \ \delta_{m+n+l, m'+n'+l'} \ . \end{aligned} \tag{2.32}$$

Similarly, the corresponding matrix element for P_3^0 can be calculated to be

$$V^{(0)}_{m'n'l'mnl} = \frac{2}{8}\sqrt{\frac{\pi}{3}}\, e^{-\frac{1}{3}(p^2-pq+q^2+r^2-rs+s^2)}\, \delta_{m+n+l,m'+n'+l'} \ . \tag{2.33}$$

Matrix elements (2.32) and (2.33) are equivalent to the expressions given for the Gaffnian Hamiltonian given in Eq. (2.17) and in Ref. [83] up to a κ-dependent normalization which we have omitted in the single-particle states. The only difference is, these matrix elements are expressed in a different set of variables which can be easily transformed in to the more common center-of-mass and orbital variables that appear in Eq. (2.17).

2.2.3 Thin torus limit

We now wish to investigate a possible scenario for gapless neutral excitations similar to those of the HR state in the TT limit. Charge neutrality is a key aspect of the domain-wall type defects studied in the preceding section. Only a neutral defect is necessarily delocalized in the manner seen there, allowing for the gapless character. Charged defects would be subject to greater constraints from "center-of-mass conservation" [38] (momentum conservation around the cylinder axis). A natural neutral defect between two different Gaffnian TT ground state patterns is given by the following configuration:

$$\ldots 200200200201011011011011011 \ldots \tag{2.34}$$

The fact that the above defect is charge neutral can be seen as follows. Starting with the $200200\ldots$ ground state pattern, we may consider a pair of particles occupying the same orbital and move one member of the pair to the left neighboring orbital, and the other to the right. We then obtain Eq. (2.34) by proceeding in this way with double occupancy to the right of the original one. Such local rearrangement of charge cannot lead to a charged defect. As written, the defect should cost a finite energy, as it violates the Gaffnian "generalized Pauli principle" [37, 81] of having no more than 2 particles in any three adjacent sites. The question is if this energy cost can be fully compensated by delocalization, as was the case for the HR state. Moreover, on the torus, defects such as the above could only occur in pairs. Assuming, then, that there is some contact energy when two such defects are in proximity, unlike it is the case for a singlet pair of defects in the HR state, this could explain why a true zero energy state featuring such delocalized defects is only possible in the thermodynamic limit. This would explain why no exact zero mode wave functions are known featuring these delocalized defects, unlike in the HR case.

Alas, the above scenario does not come to pass. We will find the asymptotic energy of defects as shown in Eq. (2.34) in the TT limit using the same perturbative approach used in the preceding section. We find that, unlike in the HR case, diagonal and off-diagonal energies for this defect are of different orders of magnitude in x in the TT limit, with the positive diagonal part dominating. We thus find the energy of such defect, and numerical calculations will show that it is indeed the energy of the lowest excited state in the TT limit. Our analytic result will show that this energy does not vanish in the thermodynamic limit.

2.2.4 TT perturbation theory

Equation (2.17) describes a center of mass conserving three particle hopping process. It is useful to explicitly spell out the first few dominant processes in the TT limit:

$$
\begin{aligned}
H \sim \sum_n \Big\{ & [C+1](C_n^\dagger)^3 (C_n)^3 \\
& + [9C(1-2\kappa^2/3)^2 + 9] e^{-2\kappa^2/3} (C_n^\dagger)^2 C_{n\pm1}^\dagger (C_n)^2 C_{n\pm1} \\
& + [6C(1-2\kappa^2) + 6] e^{-\kappa^2} (C_n^\dagger)^3 C_{n\mp1} C_n C_{n\pm1} \\
& + [9C(1-8\kappa^2/3)(1-2\kappa^2/3) + 9] e^{-5\kappa^2/3} \\
& \quad C_n^\dagger (C_{n\pm1}^\dagger)^2 (C_n)^2 C_{n\pm2} \\
& + [36C(1-2\kappa^2)^2 + 36] e^{-2\kappa^2} C_{n\mp1}^\dagger C_n^\dagger C_{n\pm1}^\dagger C_{n\mp1} C_n C_{n\pm1} \\
& + [9C(1-8\kappa^2/3)^2 + 9] e^{-8\kappa^2/3} (C_n^\dagger)^2 C_{n\pm2}^\dagger (C_n)^2 C_{n\pm2} \Big\}
\end{aligned}
\tag{2.35}
$$

The four diagonal terms out of the above dominant processes penalize states having three particles in three adjacent sites. It is apparent how the Hamiltonian assigns an energy to configurations (030), (210), (111) and (201) that is large compared to (most) off-diagonal processes. A detailed analysis similar to the one carried out in Ref. [48] could show that any zero mode of this Hamiltonian is necessarily dominated, in the usual sense [37, 81], by occupation number eigenstates free of such configurations. This is of course known to be the case for the Gaffnian wave function [37, 81]. This last observation is quite generally equivalent to saying that the TT limit must be free of such configurations. In Eq. (2.34), we see that the excited state we consider has one (201) configuration. As in the preceding

section, we write

$$H = H_0 + \lambda H_1 \,, \tag{2.36}$$

where H_0 contains all diagonal terms, and H_1 contains all off-diagonal terms, and subtleties concerning spin fluctuations are now absent. We see from Eq. (2.35) that H_0 assigns an energy of order $e^{-8\kappa^2/3}$ to the (201) defect. For comparison, the ground state patterns (200) and (110) have an H_0-energy of $\mathcal{O}(e^{-18\kappa^2/3})$ and $\mathcal{O}(e^{-14\kappa^2/3})$ per unit cell, respectively. We know, however, that the energy associated with the (200) and (110) unit cells will cancel order by order in $x = \exp(-\kappa^2/3)$ in perturbation theory, since we know that the ground states corresponding to these respective TT limits have zero energy. Hence, we will for now be interested in terms of order x^8 and lower order in x, and need to worry about higher order in x only if cancellation is found at order x^8, as it did similarly happen in the HR case.

The zeroth order (in $\lambda \equiv 1$) energy of the state (2.34) can be inferred from Eq. (2.35) as

$$E_0 = \Big[9C\big(1-\kappa^2\frac{8}{3}\big)\big(1-\kappa^2\frac{8}{3}\big)+9\Big]e^{-8\kappa^2/3}\,. \tag{2.37}$$

We look for corrections at second order in λ that are also proportional to $x^8 = e^{-8\kappa^2/3}$. We first consider diagonal processes only. The relevant virtual transition is:

$$\begin{aligned} &\ldots 200200200201011011010\ldots \\ \longrightarrow &\ldots 20020020012001101101 10\ldots \end{aligned} \tag{2.38}$$

From this we obtain the following energy correction:

$$E_2 = \frac{\left|\left[9C\left(1-\kappa^2\tfrac{8}{3}\right)\left(1-\kappa^2\tfrac{2}{3}\right)+9\right]e^{-5\kappa^2/3}\right|^2}{E_0 - \left[9C\left(1-\kappa^2\tfrac{2}{3}\right)\left(1-\kappa^2\tfrac{2}{3}\right)+9\right]e^{-2\kappa^2/3}}\,. \tag{2.39}$$

At the order we are interested in, it is safe to neglect E_0 in the denominator. We see that this correction is of order x^8, thus of the same order as E_0 and of opposite sign. So far, this is similar to the HR case. Unlike in the latter, however, there is no complete cancellation between the leading orders in x in E_0 and E_2. A positive order x^8 energy therefore remains. It turns out that this energy dominates contributions from any other processes at second or higher order in perturbation theory. We have checked explicitly up to forth order perturbation theory that all other such processes contribute only higher powers in x. This is true for both diagonal processes *and* off-diagonal processes that effectively translate the defect. While the latter processes will certainly delocalize the defect in exact eigenstates, they do not affect the energy to the leading order in x. Taking into account the fact that defects of the kind considered here only occur in pairs on the torus, we have the following relation for the gap in the TT limit:

$$E_{\mathsf{gap}} \simeq 2(E_0+E_2) = \frac{648C\kappa^4}{9+C(3-2\kappa^2)^2}e^{-8\kappa^2/3}\,. \tag{2.40}$$

2.2.5 Numerics

Eq. (2.40) assumes that the defect (2.34) does indeed correspond to the lowest (thin torus) excitation of the Gaffnian parent Hamiltonian (2.17). In order to avoid having to consider

many alternatives in the same manner, we compare Eq. (2.40) to numerics carried out for $C = 1$, Fig. 2.5. The figure shows both $N = 8$ and $N = 10$ particle data. It is evident

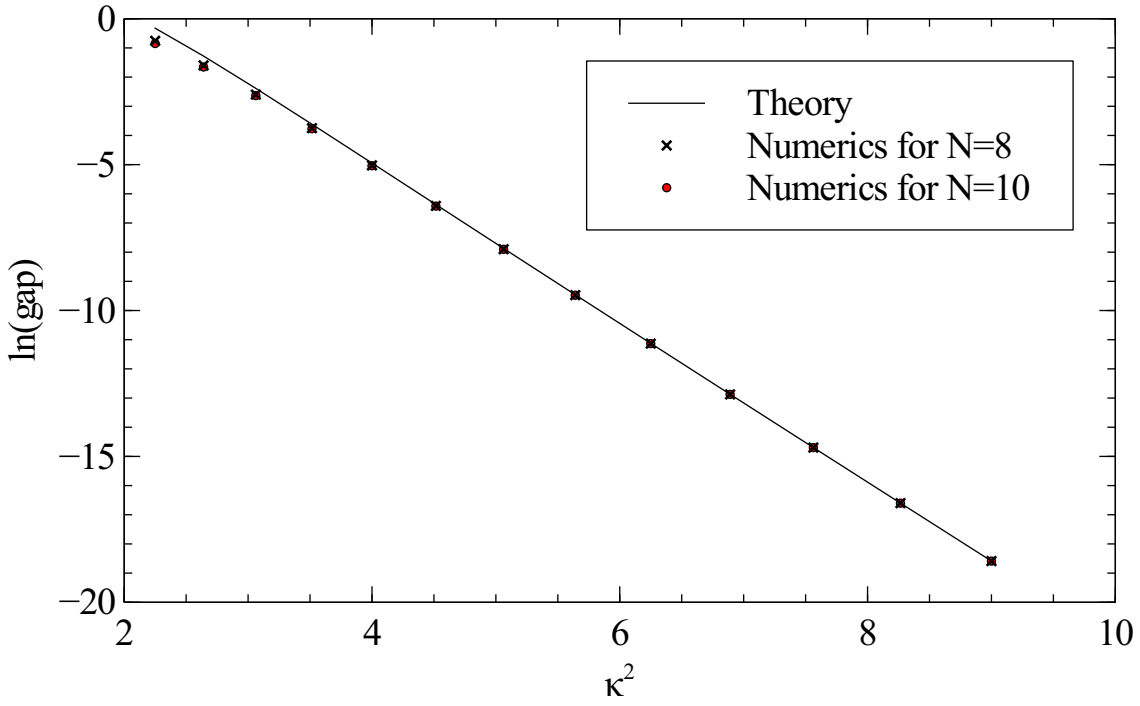

Figure 2.5: Comparison between the gap according to Eq. (2.40) (solid line) and numerical work(dots), for 8 and 10 particles. The Hamiltonian parameter C, Eq. (2.17), has been set equal to 1. We have obtained qualitatively similar results for different values of C.

that there is small discrepancy both between the $N = 8$ and the $N = 10$ particle energy gap, as well as between the latter and the prediction Eq. (2.40). Relative deviations between numerical gaps and Eq. (2.40) at $\kappa = 3$ are 0.05%. As particle number was not particularly relevant to the considerations leading to Eq. (2.40), this equation is expected to correspond to the thermodynamic (infinite cylinder) limit at *fixed* but large κ (fixed cylinder radius, small compared to a magnetic length). The $N = 8$ and $N = 10$ particle data conform to

this expectation. Also, the gap equation Eq. (2.40) was tested for different C values, and the

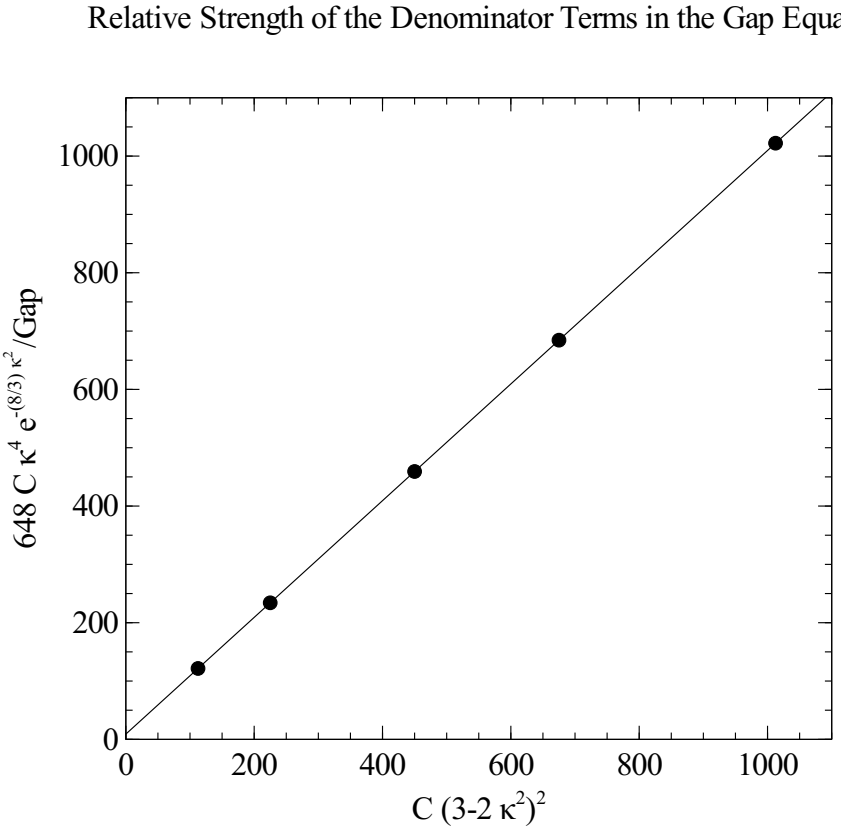

Figure 2.6: Checking the relative strength of the terms in the denominator of the gap Eq. (2.40) for different C values. Linear fit (solid line) gives an intercept and gradient of 9.0046 and 1.0006 respectively, which is in good agreement with Eq. (2.40).

relative strength of the terms in the denominator was conformed numerically as shown in Fig. 2.6. Moreover, we note that the exact first excited state has a large overlap with the state consisting of the equal amplitude superposition of all states featuring two defects of the kind shown in Eq. (2.34). For N=10 at $\kappa = 3$, the overlap between this state and the exact first

excited state is 0.999999. This confirms that we have studied the correct first excited state with our perturbative method. We thus conclude that in the $1D$ thermodynamic limit of a thin, infinite cylinder, the Gaffnian parent Hamiltonian does not have gapless excitations. Moreover, we became aware of parallel numerical work [84] where similar conclusions are reached.

2.3 Discussion and Conclusion

The perturbative scheme used here explicitly confirms the existence of gapless excitations in the TT limit of the Haldane-Rezayi state. All the results obtained here regarding this state had been anticipated earlier [47], based on the somewhat anomalous TT limit of some of the HR ground states on the torus, featuring delocalized defects. In contrast, all Gaffnian ground states have inconspicuous and simple thin torus limits. This alone could cast doubt on the existence of gapless excitations in the Gaffnian TT limit, though we have argued in Sec. 2.2.1 that such reasoning would be naive. Instead we have applied the same perturbative scheme employed in Sec. 2.1 for the HR state to the problem of thin torus Gaffnian excitation. We have identified certain charge-neutral defects as natural suspects for gapless excitations. Alas, detailed calculation has shown that these excitations are gapped, and numerics strongly suggest that they are indeed the lowest excitations in the TT limit. This implies that the 1D, thin cylinder thermodynamic limit of the Gaffnian parent Hamiltonian is gapped, unlike the similar limit for the HR parent Hamiltonian. This is similar to recent findings [85] of gapped excitations in the thin torus limit of a "fermionic analogue" of the Gaffnian state at filling factor 2/3, where, however, the underlying state corresponds to a unitary CFT. As reviewed

initially, powerful arguments suggest that both Gaffnian and HR states are gapless in the ordinary, 2D thermodynamic limit. On the torus, this opens up the interesting question of what happens if this 2D limit is approached asymmetrically, by first taking the 1D infinite cylinder limit at small cylinder radius, and subsequently taking the cylinder radius to infinity. During the latter step, gapless excitations are expected to appear, under the assumption that the 2D limit is indeed gapless. This could happen either at a critical point at some finite cylinder radius (finite κ), or only in the limit where the radius approaches infinity ($\kappa \to 0$). The latter is completely consistent with the idea of adiabatic continuity as a function of radius, at least for *any finite* radius. For this very reason, it was cautioned in Ref. [47] that finding gapless excitations in the TT limit is actually a more significant indication for their existence in the 2D limit compared to converse situation, where finding their absence in the TT limit does not necessarily imply the existence of a gap in the 2D limit, even if adiabatic continuity is assumed. The latter part of this cautionary remark seems to apply to the Gaffnian state. Barring any level crossings, it is possible that the delocalized defects identified in Sec. 2.2.1 are adiabatically connected to gapless excitations in the 2D limit. This and other interesting open questions, such as the identification of the underlying cause why gapless excitations are sometimes detectable in the TT limit and sometimes not, are left for future investigation.

Chapter 3

BOUNDS FOR LOW-ENERGY SPECTRAL PROPERTIES OF CENTER-OF-MASS CONSERVING POSITIVE TWO-BODY INTERACTIONS

A cornerstone of the theory of fractional quantum Hall liquids is the construction and study of special parent Hamiltonians that stabilize prototypical wave functions such as the Laughlin state. The properties of such Hamiltonians have been well characterized analytically where their rich structure of so-called "zero modes" is concerned, i.e., states at zero, or the lowest possible, energy. These states are of fundamental importance to the physics of a quantum Hall phase, since, in known examples, they fully describe in particular the low-energy edge physics. In contrast, very little is known rigorously about the finite-energy properties of such special Hamiltonians and their more generic deformations. This chapter reports an effort at improving this situation. Our starting point is a general monotony property, in particle number, of the ground-state energy of positive many-body Hamiltonians. We observe that the strategy leading to this result gives rise to further interesting bounds when combined with other properties of general interest in fractional quantum Hall model Hamiltonians, most importantly, center-of-mass conservation and the focus on two-body interaction. Our main result is a general bound on the step size of the ground-state energy (and in some cases the first excitation energy) with particle number. In its simplest version,

it is obtained in situations with particle-hole symmetry but is subsequently improved and generalized to situations without particle-hole symmetry, including bosons. As a special application, an upper bound on the charge gap in special model Hamiltonians with zero modes is obtained. In the latter case, we also manage to give bounds on the evolution with particle number of the first excited state by observing a certain invariance property of the zero mode subspace and then introducing a dual version thereof.

Technically, we work with second-quantized forms of projection-operator-type interactions. This is worth noting, since in this field, there is much history of deriving analytic results in a first quantized picture employing analytic wave functions [12, 33, 86] and correspondingly constructed first quantized parent Hamiltonians [12, 87]. As far as wave functions are concerned, their spectral decomposition in a particle number basis has become of interest in recent years through the study of the Jack-polynomial structure of special wave functions [37, 81] and through the more recently discovered matrix-product structure of these states [35, 36, 88]. In contrast, the use of second-quantized *Hamiltonians*, with some exceptions [74], has long been reserved for numerical work, though their popularity has recently increased as well, in part due to interest in fractional Chern insulators [83, 89–94], purely technical reasons[1] [55], as well as more general ones [48, 49, 95, 96]. The preference for first quantized descriptions of parent Hamiltonians can perhaps be attributed to the fact that these are, by construction, most suitable for studying the zero mode space, though it was recently shown (in some cases) that this is also possible in a purely second-quantized framework [48, 49, 95].

[1]Such as setting up perturbative schemes, which is possible in the thin cylinder limit [55]

Arguably, however, the advantage of working with first quantized Hamiltonians is lost when the focus is on finite-energy spectral properties. There, and moreover, when studying more generic Hamiltonians without any particularly interesting zero mode structure, arguments in favor of the greater efficiency of a "pure guiding center" description [54] are, in our opinion, particularly appealing. The second-quantized presentation of Hamiltonians is one possible way to achieve such a pure guiding center description. Our study can thus also be viewed as adding further emphasis to the utility of such an approach.

Most of the results presented below were published in Ref. [56]. However, some additional steps in certain calculations and the section 3.2.1 are added to this chapter for pedagogical reasons. Moreover, with gratitude we would like to mention that the calculations presented in section 3.2.4 were done by Tahereh Mazaheri.

3.1 Monotony of Ground State Energy

We begin by discussing the monotony in particle number and related general properties of the ground-state energy of positive many-body Hamiltonians. To attain the desired level of generality, we will first consider a second-quantized k-body interaction of the form

$$H_k = \sum_{n_1,\ldots,n_{2k}} V_{n_1\ldots n_{2k}}\, c^\dagger_{n_1}\ldots c^\dagger_{n_k} c_{n_{k+1}}\ldots c_{n_{2k}}\,. \tag{3.1}$$

The operators c_n may satisfy bosonic or fermionic commutation relations. We will later focus on the special case where a "center-of-mass" conservation law is explicit, as is appropriate for model Hamiltonians of fractional quantum Hall type systems in various geometries. For the

moment, however, the only additional property we will require is *positivity*, i.e., $\langle\psi|H|\psi\rangle \geq 0$ for all k-particle (and hence N-particle) kets $|\psi\rangle$.

We now consider an N-particle mixed state described by a density matrix ρ_N. From ρ_N, we may define various N'-particle reduced density matrices $\rho_{N'}$, $N' < N$, given recursively via

$$\rho_{N'-1} = \frac{1}{N'} \sum_n c_n \rho_{N'} c_n^\dagger \,. \tag{3.2}$$

We note that $\hat{N}\rho_{N'} = \rho_{N'}\hat{N} = N'\rho_{N'}$, where $\hat{N} = \sum_n c_n^\dagger c_n$ is the particle number operator, and $\mathrm{Tr}\,\rho_{N'-1} = \mathrm{Tr}\,\rho_{N'} = 1$. For both fermions and bosons, one easily verifies the relation

$$\hat{N}H_k = kH_k + \sum_n c_n^\dagger H_k c_n \,, \tag{3.3}$$

obtained by commuting c_n to the right. For pedagogical reasons, we present the calculation for the $2-body$ version of the above equation as the following.

We start by taking the product of the particle number operator with the 2-body Hamiltonian, and commute c_n to the right.

$$\begin{aligned}
\langle\psi|\ H_2\ |\psi\rangle &= \frac{1}{N}\ \langle\psi|\ \hat{N}H_2\ \ |\psi\rangle \\
&= \frac{1}{N} \sum_n \sum_{n_1,n_2,n_3,n_4} V_{n_1n_2n_3n_4}\ \langle\psi|\ C_n^\dagger C_n C_{n_1}^\dagger C_{n_2}^\dagger C_{n_3} C_{n_4}\ |\psi\rangle \\
&= \frac{1}{N} \sum_n \sum_{n_1,n_2,n_3,n_4} V_{n_1n_2n_3n_4} \Big[\delta_{nn_1}\ \langle\psi|\ C_{n_1}^\dagger C_{n_2}^\dagger C_{n_3} C_{n_4}\ |\psi\rangle \\
&\quad - \delta_{nn_2}\ \langle\psi|\ C_{n_2}^\dagger C_{n_1}^\dagger C_{n_3} C_{n_4}\ |\psi\rangle\ +\ \langle\psi|\ C_n^\dagger C_{n_1}^\dagger C_{n_2}^\dagger C_{n_3} C_{n_4} C_n\ |\psi\rangle \Big] \\
&= \frac{2}{N}\ \langle\psi|\ H_2\ |\psi\rangle\ +\ \mathrm{Tr}\ \rho_{N-1} H_2
\end{aligned} \tag{3.4}$$

where,

$$\rho_{N-1} \;=\; \frac{1}{N}\sum_{n} C_n \left|\psi\right\rangle \left\langle\psi\right| C_n^{\dagger} \; . \tag{3.5}$$

This gives,

$$\text{Tr}\;\rho_{N-1}H_2 \;=\; \frac{(N-1)(N-2)}{N(N-1)}\;\left\langle\psi\right|\;H_2\;\left|\psi\right\rangle \;\; . \tag{3.6}$$

Now, we can recursively perform the same calculation for the term in the left hand side of the above equation.

$$\begin{aligned}
\text{Tr}\;\rho_{N-1}H_2 \;&=\; \frac{1}{N}\sum_{n}\left\langle\psi\right| C_n^{\dagger}\, H_2\, C_n \left|\psi\right\rangle \\
&=\; \frac{1}{N(N-1)}\sum_{n}\left\langle\psi\right| C_n^{\dagger}\,\hat{N}\, H_2\, C_n \left|\psi\right\rangle \\
&=\; \frac{1}{N(N-1)}\sum_{n,m}\sum_{n_1,n_2,n_3,n_4} V_{n_1n_2n_3n_4}\left\langle\psi\right| C_n^{\dagger}\, C_m^{\dagger} C_m\, C_{n_1}^{\dagger} C_{n_2}^{\dagger} C_{n_3} C_{n_4}\, C_n \left|\psi\right\rangle \\
&=\; \frac{1}{N(N-1)}\sum_{n,m}\sum_{n_1,n_2,n_3,n_4} V_{n_1n_2n_3n_4}\Big[\delta_{mn_1}\left\langle\psi\right|\; C_n^{\dagger}\, C_m^{\dagger} C_{n_2}^{\dagger} C_{n_3} C_{n_4} C_n \;\left|\psi\right\rangle \\
&\quad -\delta_{mn_2}\left\langle\psi\right|\; C_n^{\dagger}\, C_m^{\dagger} C_{n_1}^{\dagger} C_{n_3} C_{n_4} C_n \;\left|\psi\right\rangle \;+\; \left\langle\psi\right| C_n^{\dagger}\, C_m^{\dagger}\, C_{n_1}^{\dagger} C_{n_2}^{\dagger} C_{n_3} C_{n_4}\, C_m C_n \left|\psi\right\rangle\Big] \\
&=\; \frac{2}{N-1}\;\text{Tr}\;\rho_{N-1}H_2 \;+\; \text{Tr}\;\rho_{N-2}H_2
\end{aligned} \tag{3.7}$$

where,

$$\rho_{N-2} \;=\; \frac{1}{N(N-1)}\sum_{n,m} C_m C_n \left|\psi\right\rangle \left\langle\psi\right| C_n^{\dagger} C_m^{\dagger} \tag{3.8}$$

The calculation given by Eq. (3.4) to Eq. (3.7) can be easily generalized to the $k-body$

Hamiltonians, which gives,

$$\begin{aligned}\operatorname{Tr}\rho_{N'}H_k &= \frac{1}{N'}\operatorname{Tr}\rho_{N'}\hat{N}H_k \\ &= \frac{k}{N'}\operatorname{Tr}\rho_{N'}H_k + \operatorname{Tr}\rho_{N'-1}H_k\,,\end{aligned} \tag{3.9}$$

or

$$\operatorname{Tr}\rho_{N'-1}H_k = \frac{N'-k}{N'}\operatorname{Tr}\rho_{N'}H_k\,, \tag{3.10}$$

and by induction:

$$\operatorname{Tr}\rho_{N'}H_k = \frac{(N-k)(N-1-k)\ldots(N'+1-k)}{N(N-1)\ldots(N'+1)}\operatorname{Tr}\rho_N H_k. \tag{3.11}$$

We now denote the ground-state energy of H_k in the N-particle sector as $E_0^k(N)$. Then choosing ρ_N such that $\operatorname{Tr}\rho_N H_k = E_0^k(N)$, and noting $\operatorname{Tr}\rho_{N'}H_k \geq E_0^k(N')$ by the variational principle, we have

$$E_0^k(N') \leq \frac{(N-k)(N-1-k)\ldots(N'+1-k)}{N(N-1)\ldots(N'+1)}E_0^k(N)\,. \tag{3.12}$$

So far we have not used positivity yet. A result similar to Eq. (3.12) can also be obtained for general Hamiltonians of the form

$$H = \sum_{k=k_{\mathsf{min}}}^{k_{\mathsf{max}}} H_k\,, \tag{3.13}$$

where each term represents a positive k-body interaction, with k_{min} (k_{max}) being the minimum (maximum) k. In this case we still have Eq. (3.10) for each H_k, which, for positive interaction, in particular implies

$$\mathrm{Tr}\,\rho_{N'-1}H_k \leq \frac{N'-k_{\mathsf{min}}}{N'}\ \mathrm{Tr}\,\rho_{N'}H_k\,, \tag{3.14}$$

and thus we have the same relation for H in place of H_k. For the ground-state energy within the N-particle sector $E_0(N)$, we thus obtain Eq. (3.12) with k_{min} in place of k:

$$E_0(N') \leq \frac{(N-k_{\mathsf{min}})(N-1-k_{\mathsf{min}})\ldots(N'+1-k_{\mathsf{min}})}{N(N-1)\ldots(N'+1)}E_0(N)\,. \tag{3.15}$$

Clearly, this then implies in particular the monotony of the ground-state energy with particle number,

$$E_0(N-1) \leq E_0(N)\,, \tag{3.16}$$

with equality *only* for $E_0(N)=0$. This result and a wealth of similar results all flow from Eq. (3.15) and have no doubt appeared previously in the literature, though we are unable to determine original references. For example, as another special case of Eq. (3.15), one obtaines the *superadditivity* [97] of the ground-state energy. For this consider $N'=N_1$ and $N'=N_2$ with $N_1+N_2=N$, and add the corresponding instances of Eq. (3.15):

$$E_0(N_1)+E_0(N_2) \leq ([N,N_1,k_{\mathsf{min}}]+[N,N_2,k_{\mathsf{min}}])E_0(N)\,, \tag{3.17}$$

where we have denoted the numerical factor in Eq. (3.15) as $[N,N',k]=(N-k)!N'!/(N!(N'-$

k)!). It is easy to see that $[N, N_1, k_{\mathsf{min}}] + [N, N_2, k_{\mathsf{min}}] \leq 1$. To see this, one first observes that the left-hand side is equal to 1 for $k_{\mathsf{min}} = 1$. Furthermore, $[N, N', k]$ monotonously decreases with increasing k. Hence we have the superadditivity

$$E_0(N_1) + E_0(N_2) \leq E_0(N)\,,\ N_1 + N_2 = N\,. \tag{3.18}$$

At the level of generality assumed thus far, Eq. (3.15) appears to be the strongest statement that can be made, containing a multitude of ground-state monotony properties as special cases. In the following (Section 3.2), we will be interested in a more restricted but physically relevant class of Hamiltonians that arises in particular when models of states in the fractional quantum Hall regime are considered. These Hamiltonians quite generally have an additional symmetry that in the second-quantized form Eq. (3.1) manifests itself as "center-of-mass" conservation [38]. It turns out that in this case, further bounds on the evolution of the ground-state energy with particle number can be given, and in some cases this is also true of the first excited-state energy.

3.2 Specialization to center-of-mass conserving Hamiltonians

Many known parent Hamiltonians for various types of interesting fractional quantum Hall states have a peculiar way of satisfying Eq. (3.16): the ground-state energy $E_0(N)$ is exactly zero until the particle number reaches some value $N = N_I$, where N_I/L approaches the incompressible filing factor and L is the number of Landau level orbitals available to the system due to finite size geometry (e.g. finite disk, sphere, or torus). We will comment on

the situation in the infinite disk geometry in Sec. 3.2.4, where strictly speaking, absent any other constraints, $E_0(N) = 0$ for any finite N in the case of such special model Hamiltonians. It turns out that for quantum Hall type interaction Hamiltonians, additional constraints beyond Eq. (3.15) can be given. This is chiefly due to the general presence of another symmetry, that of the conservation of the center of mass. Related to that and in addition, some models of fermions possess a particle-hole symmetry. It is then natural to surmise that in cases where Eq. (3.16) is saturated for $N < N_I$, another inequality should be saturated in the particle-hole symmetric region $N > L - N_I$. This turns out to be an *upper* bound on the step size in ground-state energy with particle number, $E_0(N) - E_0(N-1)$. This in particular provides an upper bound on the charge gap at the incompressible filling factor of special model Hamiltonians satisfying the "zero mode paradigm"

$$E_0(N) = 0 \text{ for } N \leq N_I \tag{3.19}$$

but can be applied equally well to some more generic Hamiltonians. Before we derive these and other results, we will first write the Hamiltonian in a form in which all its pertinent properties are manifest.

In a constant magnetic background field, Landau-level projection leads to a one-dimensional "lattice" Hilbert space of single-particle orbitals labeled by an integer guiding center quantum number n, whose precise meaning depends on the geometry and choice of basis. Here, these orbitals are created by the operators $c_n^\dagger$. Certain rotational and or (magnetic) translational symmetries manifest themselves as "center-of-mass conservation", i.e., the matrix

element in Eq. (3.1) is non zero only when $n_1 + \ldots n_k = n_{k+1} + \ldots + n_{2k}$ is satisfied (on the torus modulo L). This can be made manifest by writing the Hamiltonian (3.13) in the form

$$H = \sum_{m=1}^{M} \sum_{r=0}^{k_m - 1} \sum_{R \in \mathbb{Z} + r/k_m} Q_R^{m\dagger} Q_R^m \,, \tag{3.20a}$$

where

$$Q_R^m = \sum_{n_1, \ldots, n_{k_m}} \eta^m_{R; n_1, \ldots, n_{k_m}} c_{n_1} \cdots c_{n_{k_m}} \,. \tag{3.20b}$$

Eq. (3.20) can be obtained from Eqs. (3.13) and (3.1) by performing a spectral decomposition of the symbol $V_{n_1 \ldots n_{2k}}$, viewed as a big matrix with multi-indices $(n_1, \ldots, n_k)$ and $(n_{k+1}, \ldots, n_{2k})$. This matrix is block-diagonal in multi-indices of given $R = (n_1 + \ldots + n_k)/k$, and so eigenvectors $\eta^m_{R; n_1 \ldots n_k}$ can be labeled by R. These eigenvectors are normalized such that $\sum_{\{n_i\}} |\eta^m_{R; n_1 \ldots n_k}|^2$ equals the corresponding eigenvalue, and the absence of negative coefficients signifies the positivity of the Hamiltonian. In Eq. (3.20), M different terms labeled by m are considered, each of which corresponds to an eigenvector of the aforementioned kind, obtained for a k_m-body operator in Eq. (3.13), with non zero eigenvalue. To establish full equivalence between Eqs. (3.13) and (3.20), the case $M = \infty$ must be considered, whereas often M will be finite in quantum Hall model Hamiltonians. In the following, we will refer to the Hamiltonian either in the form (3.20) or in the less explicit but more condensed form Eqs. (3.1), (3.13), whichever is more convenient. We note that when working on the torus, center-of-mass conservation strictly holds only "modulo L". In this case we will still take the Hamiltonian to be of the form Eq. (3.20), where $c_n \equiv c_{n+L}$, and all symbols $\eta^m_{R; n_1 \ldots n_k}$ are

likewise invariant under the shift $n_i \to n_i + L$.

3.2.1 Example: Monotony property of the "Special" Hamiltonians in the spherical geometry

Here, we will give an alternative derivation of the monotony property for the special case of systems with spherical symmetry. Although this case is already fully covered by the more general result derived in the preceding section, the heavy use of symmetry properties we will make in this alternative derivation will lead to intermediate results that will be very useful in the remainder of this thesis. As discussed in Chapter 1, using the spherical geometry is sometimes convenient in studying the bulk properties of FQH effect due to the finite Landau level degeneracy and the non-existence of edges. This subsection can also serve as a pedagogical introduction to a formalism in the sphere.

Let's consider a sphere with a radially outward magnetic field. Let's take the total flux piercing through the sphere to be N_ϕ. The orbitals (or single particle states) of the lowest Landau level (LLL) will transform under a spin $N_\phi/2$ representation of $SU(2)$. Let's take $L(= N_\phi + 1)$ to be the number of available single particle states, and N to be the total number of particles in the system.

In order to preserve the generality, ground state $|\psi\rangle$ in the N-particle sector will be considered to be a multiplet, $|\psi_m\rangle$ with $m = -s, ..., s$; where s being the corresponding angular momentum quantum number of the multiplet. In the following we will also assume that the Q_R of Eq. (3.20) transforms under a unitary representation of $SU(2)$. This is tantamount to assuming that the Hamiltonian Eq. (3.20) is rotationally invariant. Note that

we specialized to one "flavor" of Q_R operators and so have dropped the label m from Q_R in Eq. (3.20). The generalization to M labels is trivial. The proof of the following two lemmas will be needed to prove the monotony property.

1. $\sum_m \langle\psi_m| C_n^\dagger C_n |\psi_m\rangle$ is independent of n.

2. $\sum_R \sum_m \langle\psi_m| Q_R^\dagger C_n^\dagger C_n Q_R |\psi_m\rangle$ is independent of n.

To this end, we follow a group theoretic argument as shown below.

1. $\sum_m \langle\psi_m| C_n^\dagger C_n |\psi_m\rangle$ ***is independent of n.***

Since the N-particle ground state belongs to a multiplet $|\psi_m\rangle$, let's consider the following matrix element:

$$M_{nn'} = \sum_m \langle\psi_m| C_n^\dagger C_{n'} |\psi_m\rangle = \mathrm{Tr}\left[\sum_m |\psi_m\rangle \langle\psi_m| C_n^\dagger C_{n'}\right] , \tag{3.21}$$

where, the trace is over the entire LLL Fock space. Now, consider the new basis,

$$|\psi_{m'}\rangle = \underbrace{e^{i\alpha S^j}}_{U_j(\alpha)} |\psi_m\rangle \ , \tag{3.22a}$$

with,

$$U_{mm'} = \langle\psi_m| U_j(\alpha) |\psi_{m'}\rangle \ , \tag{3.22b}$$

being a unitary matrix. Here, S^j with $j = x, y, z$ are the generators of $SU(2)$-rotations. The $|\psi_m\rangle$'s form a $U_j(\alpha)$-invariant subspace, so the projection operator given below is invariant

under $U_j(\alpha)$:

$$\sum_m U_j(\alpha)\,|\psi_m\rangle\,\langle\psi_m|\,U_j(\alpha)^\dagger = \sum_{m'} |\psi_{m'}\rangle\,\langle\psi_{m'}|\ . \tag{3.23}$$

That is, the projection operator, $\sum_m U_j(\alpha)\,|\psi_m\rangle\,\langle\psi_m|\,U_j(\alpha)^\dagger$ is the identity in the subspace in consideration. Now, insert $U_j(\alpha)$'s in Eq. (3.21) and expand for small α. Matrix elements $M_{nn'}$ should be independent of α. Therefore, the resulting terms should be zero in order by order in α:

$$\begin{aligned}
M_{nn'} &= \mathrm{Tr}\Big[\Big(1 + i\alpha S^j + ...\Big) \\
&\times \sum_m |\psi_m\rangle\,\langle\psi_m|\,\Big(1 - i\alpha S^j + ...\Big) C_n^\dagger\, C_{n'}\Big] \\
&= M_{nn'} + i\alpha\,\mathrm{Tr}\Big[\sum_m |\psi_m\rangle\,\langle\psi_m|\,C_n^\dagger\, C_{n'} S^j \\
&- \sum_m |\psi_m\rangle\,\langle\psi_m|\,S^j C_n^\dagger\, C_{n'}\Big] + ... \\
&= M_{nn'} + i\alpha\,\mathrm{Tr}\Big(\sum_m |\psi_m\rangle\,\langle\psi_m|\,[C_n^\dagger\, C_{n'}, S^j]\Big) + ...\ .
\end{aligned} \tag{3.24}$$

In the second line of the above calculation, the S^j operator was moved cyclically inside the trace. Now let's use the following definition considering the fact that C_n operators transform under a spin $N_\phi/2$ representation of $SU(2)$:

$$[S^j, C_n] = \sum_{n''} S^j_{n'',n} C_{n''}\ , \tag{3.25}$$

and the adjoint,

$$-[S^j, C_n^\dagger] \;=\; \sum_{n''} S^{j*}_{n,n''} C^\dagger_{n''} \;, \tag{3.26}$$

where, $S^j_{n'',n}$ is a Hermitian matrix and "$*$" denotes the complex conjugation. The commutator appearing in the last line of Eq. (3.24) can be calculated as below:

$$\begin{aligned}
[C_n^\dagger\, C_{n'}, S^j] &= [C_n^\dagger, S^j] C_{n'} + C_n^\dagger [C_{n'}, S^j] \\
&= -[S^j, C_n^\dagger] C_{n'} - C_n^\dagger [S^j, C_{n'}] \\
&= \sum_{n''} S^{j*}_{n,n''}\, C^\dagger_{n''} C_{n'} - C_n^\dagger \sum_{n''} S^j_{n'',n'} C_{n''} \\
&= \sum_{n''} \Big(S^{j*}_{n,n''}\, C^\dagger_{n''} C_{n'} - C_n^\dagger C_{n''}\, S^j_{n'',n'} \Big) \;.
\end{aligned} \tag{3.27}$$

This result can be substituted in Eq. (3.24) instead for the commutator $[C_n^\dagger\, C_{n'}, S^j]$. Moreover, notice that $S^{j\dagger} = S^j$, where $S^{j\dagger}$ is the Hermitian conjugate of the Hermitian matrix, S^j. We can use this fact in Eq. (3.24) as shown below:

$$\begin{aligned}
M_{nn'} &= M_{nn'} + i\alpha\, \mathrm{Tr} \Big(\sum_m |\psi_m\rangle \langle\psi_m| \, [C_n^\dagger\, C_{n'}, S^j] \Big) + ... \\
&= M_{nn'} + i\alpha\, \mathrm{Tr} \Big(\sum_m |\psi_m\rangle \langle\psi_m| \\
&\times \;\; \Big(\sum_{n''} (S^{j*}_{n,n''}\, C^\dagger_{n''} C_{n'} - C_n^\dagger C_{n''}\, S^j_{n'',n'}) \Big) \Big) + ... \\
&= M_{nn'} + i\alpha \Big(\sum_{n''} (S^{j*}_{n,n''} M_{n'',n'} - M_{n,n''} S^j_{n'',n'}) \Big) + ... \\
&= M_{nn'} + i\alpha \Big((S^{j\dagger} M)_{n,n'} - (M S^j)_{n,n'} \Big) + ... \\
&= M_{nn'} + i\alpha \Big((S^j M)_{n,n'} - (M S^j)_{n,n'} \Big) + ... \\
&= M_{nn'} - i\alpha [M_{nn'}, S^j_{nn'}] + ... \;.
\end{aligned} \tag{3.28}$$

As mentioned above, the resulting terms should be zero order by order in α. Therefore, Eq. (3.28) implies that $[M_{nn'}, S^j_{nn'}] = 0$. But, $S^j_{nn'}$ is a finite dimensional irreducible representation. This allows us to use Schur's lemma and deduce that,

$$M_{nn'} \propto \mathbb{1} \Rightarrow indep.\, of\, n \tag{3.29}$$

In particular, this proves that $\langle\psi_m| C^\dagger_n C_n |\psi_m\rangle$ are independent of n and the off-diagonal matrix elements are zero. Thus the lemma is proven.

Proof: $\sum_R \sum_m \langle\psi_m| Q^\dagger_R C^\dagger_n C_n Q_R |\psi_m\rangle$ ***is independent of n.*** Recall that we assume that Q_R belong to a representation that is unitary. Since this is also true for the $|\psi_m\rangle$ the product $Q_R |\psi_m\rangle$ will also transform under a unitary representation. The above proof for $lemma - 1$ therefore carries without change.

Now, notice that $Q_R |\psi\rangle$ will be a state with $(N-2)$ number of particles. We then have $\sum_m \langle\psi_m| Q^\dagger_R \hat{N} Q_R |\psi_m\rangle = (N-k) \sum_m \langle\psi_m| Q^\dagger_R Q_R |\psi_m\rangle$, where Q_R destroys k fermions. This allows us to write

$$\frac{\sum_R \sum_n \sum_m \langle\psi_m| Q^\dagger_R C^\dagger_n C_n Q_R |\psi_m\rangle}{\sum_R \sum_m \langle\psi_m| Q^\dagger_R Q_R |\psi\rangle} = (N-k)\ . \tag{3.30}$$

Now, using the fact that, $\sum_R \sum_m \langle\psi_m| Q^\dagger_R C^\dagger_n C_n Q_R |\psi_m\rangle$ is independent of n, we can replace the n-sum by factor L, which gives

$$\frac{\sum_m \langle\psi| C^\dagger_n \sum_R Q^\dagger_R Q_R C_n |\psi\rangle}{\sum_m \langle\psi| Q^\dagger_R \sum_R Q_R |\psi\rangle} = \frac{(N-k)}{L}\ . \tag{3.31}$$

where, we have used the commutation relation $[Q_R, C_n] = 0$, and its adjoint.

In the same way we also derive

$$\frac{\sum_m \langle\psi_m| C_n^\dagger C_n |\psi_m\rangle}{\sum_m \langle\psi_m|\psi_m\rangle} = \frac{N}{L} \ . \tag{3.32}$$

Combining Eq. (3.31) and Eq. (3.32) gives

$$\frac{\sum_m \langle\psi| C_n^\dagger \sum_R Q_R^\dagger Q_R C_n |\psi\rangle}{\sum_m \langle\psi| \sum_R Q_R^\dagger Q_R |\psi\rangle} = \Big(\frac{N-k}{N}\Big) \frac{\sum_m \langle\psi_m| C_n^\dagger C_n |\psi_m\rangle}{\sum_m \langle\psi_m|\psi_m\rangle} \ . \tag{3.33}$$

Rearrangement of terms leads to

$$\frac{\sum_m \langle\psi| C_n^\dagger \sum_R Q_R^\dagger Q_R C_n |\psi\rangle}{\sum_m \langle\psi_m| C_n^\dagger C_n |\psi_m\rangle} = \Big(\frac{N-k}{N}\Big) \frac{\sum_m \langle\psi| \sum_R Q_R^\dagger Q_R |\psi\rangle}{\sum_m \langle\psi_m|\psi_m\rangle} \ . \tag{3.34}$$

The summations over R values in the above expressions are for integer and half odd integer values. Therefore, we can use $H = \sum_R Q_R^\dagger Q_R$ to get the final expression

$$\frac{\sum_m \langle\psi_m| C_n^\dagger H C_n |\psi_m\rangle}{\sum_m \langle\psi_m| C_n^\dagger C_n |\psi_m\rangle} = \Big(\frac{N-k}{N}\Big) \frac{\sum_m \langle\psi_m| H |\psi_m\rangle}{\sum_m \langle\psi_m|\psi_m\rangle}, \tag{3.35}$$

where, H being the Hamiltonian. Eq.(3.35) is a variational statement of the monotony of the ground state in the spherical geometry in the following way. We can define the N-particle and $(N-1)$-particle density operators as

$$\rho_N = \frac{\sum_m |\psi_m\rangle \langle\psi_m|}{\sum_m \langle\psi_m|\psi_m\rangle} \ , \tag{3.36a}$$

and,

$$\rho_{N-1} = \frac{\sum_m C_n \left|\psi_m\right\rangle \left\langle\psi_m\right| C_n^\dagger}{\sum_m \left\langle\psi_m|C_n^\dagger C_n|\psi_m\right\rangle} \ , \tag{3.36b}$$

respectively. Eq. (3.35) now reads as

$$\mathrm{Tr}\, \rho_{N-1} H = \Big(\frac{N-k}{N}\Big)\, \mathrm{Tr}\, \rho_N H \ . \tag{3.37}$$

We now denote the ground-state energy of H in the N-particle sector as $E_0(N)$. Then choosing ρ_N such that $\mathrm{Tr}\, \rho_N H = E_0(N)$, and noting $\mathrm{Tr}\, \rho_{N-1} H \geq E_0(N-1)$ by the variational principle, we have

$$E_0(N-1) \leq \frac{(N-k)}{N} E_0(N)\,. \tag{3.38}$$

Thus the monotony property is proven in the spherical geometry.

3.2.2 Particle-hole symmetry

We will now demonstrate that the results already established have further powerful implications on the evolution of the lowest eigenvalue with particle number in the presence of center-of-mass conservation as discussed in section 3.2. A strikingly simple special instance of this is the case of $k = 2$-body interactions for fermions. In this case, the spatial symmetries of the problem often also imply a particle-hole symmetry, as we will now discuss.

We introduce the charge conjugation operator as a linear unitary operator C defined via $C c_n C = c_n^\dagger$, where $C = C^\dagger$, or $C^2 = \mathbb{1}$. Consider now a two-body Hamiltonian H_2 as given in Eq. (3.1), and assuming that the interaction matrix element V_{n_1,n_2,n_3,n_4} is proportional to

$\delta_{n_1+n_2,n_3+n_4}$, easy calculation gives

$$CH_2C = 2\sum_n \Delta_n - 4\sum_n \Delta_n c_n^\dagger c_n + H_2\,, \tag{3.39a}$$

where

$$\Delta_n = \sum_m V_{mnnm} \tag{3.39b}$$

We emphasize that even though there is no strict center-of-mass conservation on the torus, but only "modulo L", Eq. (3.39) is also obtained on the torus where the operators and η–form-factors have the aforementioned periodicity. Specifically, if we write a *translationally invariant* two-body interaction on the torus in the form (3.20) via

$$Q_R^m = \frac{1}{2}\sum_x \eta^m(x) c_{R-x} c_{R+x}\,, \tag{3.40}$$

where x runs over integer (half-odd-integer) values in the interval $[0, L)$ for integer (half-odd-integer) R, and $\eta^m(x)$ satisfies $\eta^m(x+L) = \eta^m(x)$ along with, for fermions, $\eta^m(x) = -\eta^m(-x)$, we find

$$\Delta_n = \frac{1}{4}\sum_m \sum_{x\in\frac{1}{2}\mathbf{Z}} |\eta^m(x)|^2 \equiv \Delta, \tag{3.41}$$

where the sum is over all integer *and* half-odd-integer values in $[0, L)$. In particular, it is apparent that $\Delta_n \equiv \Delta$ does not depend on n at all. The same result holds in the presence

of spherical symmetry as discussed in section 3.2.1 (lemma-1) and Ref. [98]

$$\Delta_n \equiv \Delta = \frac{1}{L}\sum_{m,n} V_{mnnm}\,. \tag{3.42}$$

We thus write Eq. (3.39) in its final form,

$$CH_2C = 2\Delta L - 4\Delta\hat{N} + H_2\,, \tag{3.43}$$

which directly relates the spectrum at particle number N to that at $L-N$. We read off:

$$E_0(N) = E_0(L-N) + (4N-2L)\Delta\,. \tag{3.44}$$

Eq. (3.44) applies not only to the ground-state energy but to the entire spectra at N and $L-N$, respectively, and is the manifestation of particle-hole symmetry of fermionic two-body interactions on the sphere or torus. Figure 3.1 shows our current understanding of the spectrum of a "special" Hamiltonian. The following results will improve on this situation. It is straightforward to combine this last equation with the monotony result Eq. (3.16) into a new bound on the step size of energy with particle number:

$$E_0(N+1) - E_0(N) \leq 4\Delta\,. \tag{3.45}$$

In the thermodynamic limit, this in particular constrains the chemical potential at zero temperature. We emphasize, however, that the validity of Eq. (3.45) is not limited to large

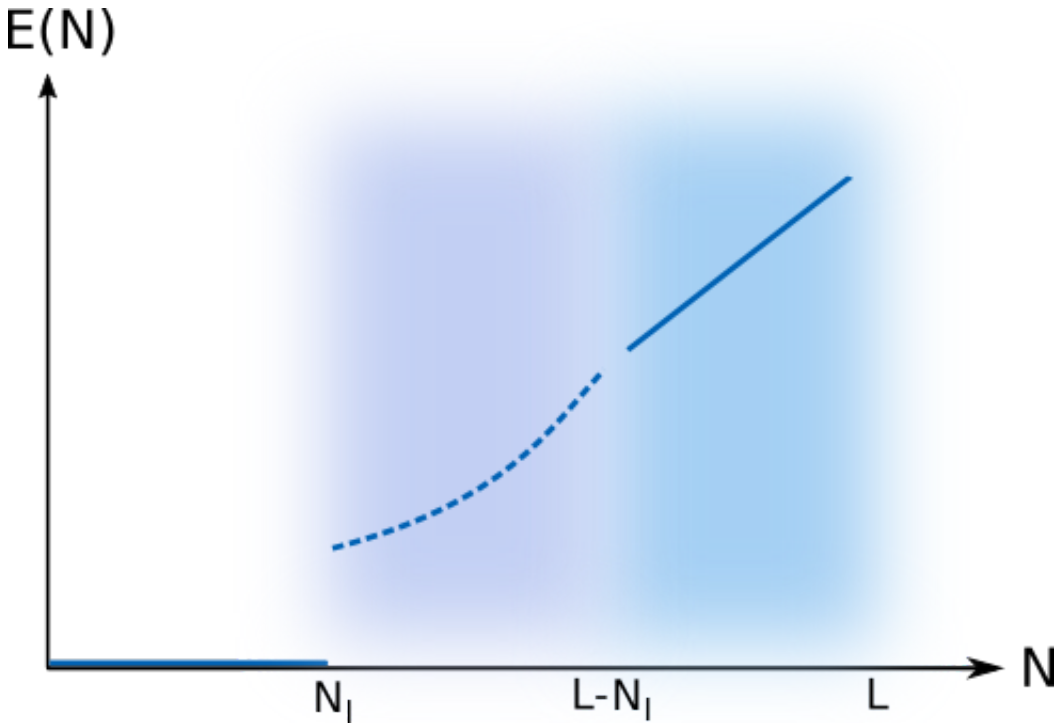

Figure 3.1: Schematic variation of ground state energy of a "special" Hamiltonian according to the knowledge prior to the current project. Nothing much is rigorously known in the region shown in purple (dashed line). L is the number of lowest Landau level orbitals available. Ground state energy is zero until N_I ("incompressible particle number") which is $L/3$ for Laughlin 1/3 state.

system size. Also, we will in the following derive similar relations that can be applied to excitations. Hence we will refer to the quantity on the left-hand side of this equation by the more generic term "energy step size" in the following.

Some remarks are in order to demonstrate that the above result is meaningful. We may, for example, consider the V_1 Haldane pseudopotential on the torus, with coefficients normalized such that

$$\frac{1}{2} \sum_{x \in \mathbf{Z} \text{ or } x \in \mathbf{Z}+\frac{1}{2}} |\eta^1(x)|^2 \doteq 1 \,, \tag{3.46}$$

as befits a projection operator. (note double counting due to the fact that x and $-x$ lead to identical terms in Eq. (3.40).) The $\doteq$ symbol signifies that on the torus, small deviations from the value of 1 appear due to the standard periodization of pseudopotentials, which vanish in the thermodynamic limit and are not present on the sphere. In either case, in the thermodynamic limit, Eq. (3.41) gives $\Delta = 1$, owing to the fact that now x runs over both integer and half-odd-integer values. In particular, the right-hand side of Eq. (3.45) is of order unity.

Moreover, we observe that the inequality Eq. (3.45) may be saturated. If we sum over the first M odd Haldane pseudopotentials, it is well known [12] that the resulting Hamiltonian satisfies Eq. (3.19) with N_I approaching $L/(M+1)$. From Eq. (3.44), it is then clear that in this case,

$$E_0(N) = (4N - 2L)\Delta \ , \quad \text{for } N \geq L - N_I \, . \tag{3.47}$$

Therefore, Eq. (3.45) is the best possible bound on the energy step size that is uniform in N. Below we will see that a slight improvement is possible at the expense of bringing in more complicated, N-dependent coefficients. The main benefit of the following considerations is, however, their greater generality. We finally remark that the single-particle charge gap may be defined as $\Delta_c = E_0(N+1) + E_0(N-1) - 2E_0(N)$. For the special (Laughlin state) parent Hamiltonians discussed above, the energy then jumps from $E(N \leq N_I) = 0$ to the charge gap $E(N_I + 1) \equiv \Delta_c$ at the incompressible filling factor, and we have in particular obtained an upper bound on this charge gap:

$$\Delta_c \leq 4\Delta\,. \tag{3.48}$$

We note that this last relation is, in its functional form, reminiscent of results obtained via the "single mode appimationroximation" [99, 100]. However, it essentially complements the latter, which provides a variational upper bound on the *neutral* gap. It is further worth pointing out that the above was obtained solely by appealing to the two principles of ground-state monotony and particle-hole symmetry, bypassing the need for the construction of clever variational wave functions.

3.2.3 Bosons, excited states, and duality

The bound Eq. (3.45) has the advantage of simplicity. However, some limitations thus far apply. So far, we have only considered particle-hole symmetric two-body interactions of fermions. Interestingly, a road to generalization of this result manifests itself if we first limit our attention to special model Hamiltonians and inquire about the evolution, in N, of the first excited state for such N where zero modes are present (and the ground-state energy thus vanishes exactly). It turns out that this question can be investigated with methods similar to those of Sec. 3.1, thanks to the following fortuitous circumstance. It has been pointed out that the zero mode space $\mathcal{H}_Z$ of the Hamiltonian is generally invariant under the action of destruction operators c_n (see, e.g., Refs. [49, 95]). Indeed, this follows from the zero mode condition $Q_R^m\,|\psi\rangle = 0$ for all n, R, and from the commutation relation $[Q_R^m, c_n] = 0$. Much less appreciated seems to be the fact that there is a dual version of this statement. Let

$\mathcal{H} = \mathcal{H}_Z \oplus \mathcal{H}_{NZ}$ be the decomposition of the Hilbert space into the zero mode subspace and its orthogonal complement, the latter being spanned by all finite-energy eigenstates. Then in fact $\mathcal{H}_{NZ}$ is invariant under the action of all creation operators $c_n^\dagger$. For, if $|\psi\rangle \in \mathcal{H}_{NZ}$, and $|\phi\rangle$ is any zero mode, then $c_n |\phi\rangle$ is also a zero mode. Thus $\langle\psi|c_n|\phi\rangle = 0 = \langle\phi|c_n^\dagger|\psi\rangle$. So $c_n^\dagger |\psi\rangle$ is orthogonal to any zero mode. Thus $c_n^\dagger |\psi\rangle \in \mathcal{H}_{NZ}$ if $|\psi\rangle$ is.

We now consider $E_1(N, L)$, the lowest *non zero* eigenenergy for given particle number N, where in the following, we will make both the N and the L dependence explicit. Note that for such N where there are no zero modes, $E_1(N, L) = E_0(N, L)$, and the following considerations equally apply to this situation. In general, $E_1(N, L)$ is the ground-state energy of $\mathcal{H}_{NZ}$ for fixed N, and the invariance of $\mathcal{H}_{NZ}$ under the creation operators $c_n^\dagger$ allows us to proceed in a manner that parallels the considerations of Sec. 3.1, except stepping up in particle number instead of stepping down.

To this end, we restrict ourselves for now to two-body interactions of fermions, which we simply denote by $H_2 \equiv H$ below. For such interactions, we note the identity

$$(L - \hat{N})H = \sum_n c_n c_n^\dagger H = 2H - 4\Delta\hat{N} + \sum_n c_n H c_n^\dagger \,, \tag{3.49}$$

where again center-of-mass conservation and symmetries have been used to extract the term Δ, Eq. (3.42). It is then straightforward to proceed along the lines of Eqs. (3.3)-(3.15), where only the concept of a reduced density matrix Eq. (3.2) must be replaced by a dual

counterpart of an "enlarged" (in particle number) density matrix,

$$\rho_{N'+1} = \frac{1}{L-N'} \sum_n c_n^\dagger \rho_{N'} c_n \,. \tag{3.50}$$

This then leads to the relation

$$E_1(N+1,L) - \frac{L-N-2}{L-N} E_1(N,L) \leq \frac{4N}{L-N} \Delta \,. \tag{3.51}$$

We emphasize once more that Eq. (3.51) describes both the first excited-state energy in the presence of zero modes, as well as, in the absence of the latter, the ground-state energy. As far as this second application is concerned, it is quite similar to Eq. (3.45), as the coefficient on the left-hand side is close to unity for large $L-N$, and the bound on the left-hand side even represents an improvement over Eq. (3.45) for $N < L/2$. One may again check that Eq. (3.51) is saturated in the regime discussed in and around Eq. (3.47).

Eq. (3.51) has been derived by taking the expectation value of Eq. (3.49) in the ground state of $\mathcal{H}_{NZ}$. If instead we again consider $N = N_I$, the largest N for which $E_0(N,L) = 0$, and take the expectation value of Eq. (3.49) for the corresponding zero mode ground state, we obtain the following upper bound on the charge gap:

$$\Delta_c \leq \frac{4N_I}{L-N_I} \Delta \,, \tag{3.52}$$

which is usually (for $N_I/L < 2$) an improvement over Eq. (3.48). We can revisit Figure 3.1

to complete it with our new results as shown in Figure 3.2.

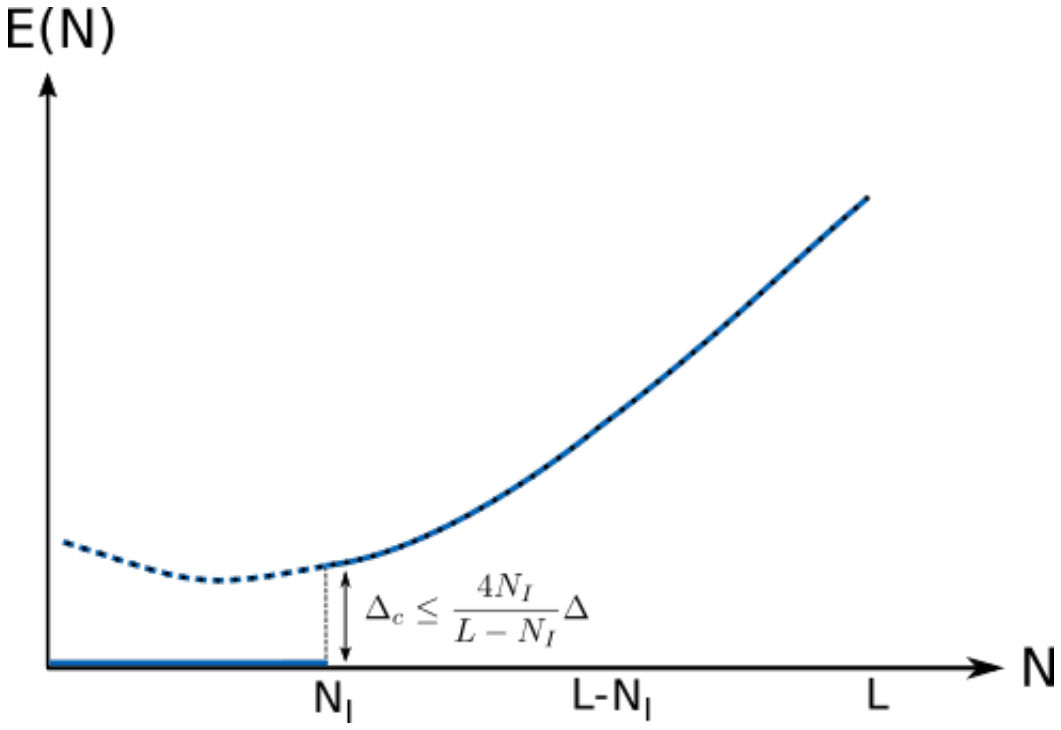

Figure 3.2: Schematic variation of ground state energy of a "special" Hamiltonian. Upper bounds for the "charge gap" and energy step size (at black dots) for the ground state energy and the first excited state energy has been proved. L is the number of lowest Landau level orbitals available. Ground state energy is zero until N_I ("incompressible particle number") which is $L/3$ for Laughlin 1/3 state.

We emphasize that while in deriving Eq. (3.49), we used the same symmetries that lead to particle-hole symmetry for fermions, particle-hole symmetry does itself not seem to play any essential role here. To make this point, we now derive analogous results for two-body interactions of bosons. In this case, the analog of Eq. (3.49) is given by

$$(L+\hat{N})H = -2H - 4\Delta\hat{N} + \sum_n c_n H c_n^\dagger \,. \tag{3.53}$$

This then leads in an analogous manner to

$$E_1(N+1,L) - \frac{L+N+2}{L+N} E_1(N,L) \leq \frac{4N}{L+N}\Delta\,. \tag{3.54}$$

This is again similar in spirit to the "step size" equation (3.45), and, in addition to generalizing the latter to bosons, has the same benefit as Eq. (3.51), applying also to the first excited state in the presence of zero modes. We may now further generalize Eq. (3.52) to bosons via

$$\Delta_c \leq \frac{4N_I}{L+N_I}\Delta\,. \tag{3.55}$$

We note one more subtle difference between Eqs. (3.51) and (3.54). In Eq. (3.51), the positive term $2E_1/(L-N)$ may always be dropped if desired, in order to bound the step size more directly. This is not immediately possible in Eq. (3.54), where a similar term appears with opposite sign. While this term appears innocent at first, it gets somewhat out of control when E_1 approaches order L. *A priori*, we do not know when that happens. However, it is easy enough to use Eq. (3.54) in order to bound $E_1(N,L)$ directly. To demonstrate this, let us focus on the region $N > N_I$. In this case, we prove from Eq. (3.54) by easy induction that

$$E_1(N,L) \leq \frac{2N(N-1)}{L+1}\Delta \quad (N > N_I)\,, \tag{3.56}$$

using Eq. (3.55) with $N = N_I + 1$ as the starting point of the induction. It is clear that Eq. (3.56) may be much improved if N_I is appreciably larger than 1. Proceeding with the

general Eq. (3.56), however, we in particular see that

$$E_0(N, L) \leq 2L\Delta \quad (N < L)\,, \tag{3.57}$$

where we note again that E_1 and E_0 are defined to be the same for $N > N_I$. This in Eq. (3.54) actually reproduces the original step size equation (3.45), now for bosons, with the additional restriction of $N \leq L$, i.e., filling factor no greater than 1.

In closing this section, we evaluate the bound (3.52) for the important special case of the V_1 Haldane pseudopotential on a sphere threaded by $N_\Phi = L-1$ flux quanta, which stabilizes a $\nu = 1/3$ Laughlin state of N_I particles, where $N_\Phi = 3(N_I - 1)$. Table 3.1 summarizes our results. Note that as defined above in Eq. (3.48), the charge gap Δ_c corresponds to a state of $N = N_I + 1$ particles or the insertion of three quasi-particles into the Laughlin state, which must be well separated before the thermodynamic limit is reached. While this is not quite the case for the system sizes shown in Table 3.1 yet, we emphasize that the bounds derived here apply equally well to finite particle number. Moreover, one may be confident from the data given that even in the thermodynamic limit, our upper bound Eq. (3.52) overestimates the charge gap by less than a factor of 2. This seems quite reasonable, given the great generality of the bounds derived here. As we stressed above, these bounds are saturated in certain cases; hence there is not much room for improvement at this level of generality. In this light, the fact that Eq. (3.52) is within less than a factor of 2 of the actual gap seems quite satisfactory.

N	L	Δ	$(\Delta_c)_{ub}$	$(\Delta_c)_{ED}$	$\frac{(\Delta_c)_{ub}}{(\Delta_c)_{ED}}$
5	10	0.8500	2.2667	1.6406	1.38
6	13	0.8846	2.2115	1.4600	1.52
7	16	0.9063	2.1750	1.4208	1.53
8	29	0.9211	2.1491	1.3692	1.57
9	22	0.9318	2.1299	1.3367	1.60
10	25	0.9400	2.1150	1.3100	1.62

Table 3.1: Charge gap for a sphere threaded by $N_\Phi = L-1$ flux quanta, at the incompressible filling factor of the V_1 Haldane pseudopotential (see text). N represents particle number, the parameter Δ defined by Eq. (3.42) equals $1 - 3/(2L)$ for the V_1 pseudopotential, $(\Delta_c)_{ub}$ is the upper bound on the charge gap as given by Eq. (3.52), and $(\Delta_c)_{ED}$ is the actual charge gap as determined by exact diagonalization.

3.2.4 Considerations for the disk

Most of the above results, except for the general monotony Eq. (3.16), are not in any obvious way applicable or sensible in the infinite disk geometry, where $L = \infty$. In this case, the Hilbert space of any rotationally invariant Hamiltonian nonetheless decomposes into finite dimensional subspaces of given particle number N *and* given angular momentum $\mathcal{L}_z$. The lowest energy $E_0(N, \mathcal{L}_z)$ then satisfies a fairly obvious monotony relation in the angular momentum variable $\mathcal{L}_z$, which we wish to mention here for completeness.

In the disk geometry, a decomposition into center of mass and relative degrees of freedom is possible, and any Hamiltonian with translational and rotational invariance will decouple from the center-of-mass degrees of freedom. In this context, it is useful to introduce ladder operators a_i, $a_i^\dagger$, $[a_i, a_j^\dagger] = \delta_{ij}$ such that $a_i^\dagger a_i$ is the angular momentum of the i th particle. We stress that these operators are very different from the "second-quantized" operators c_n,

which carry orbital indices and preserve the symmetry of the wave function. In contrast, the a_i carry particle indices like any first quantized single-particle operators, thus not by themselves preserving the symmetry of the wave function, which is also not in any way encoded in the commutation relations of the a_i. As a result, the following is independent of particle statistics.

In this description, the relative degrees of freedom are (over-)completely described by the operators $a_i - a_j$ and their Hermitian adjoints. The total angular momentum operator may be decomposed into a center-of-mass part and a relative part, respectively, via

$$\mathcal{L}_z = \mathcal{L}_z^{\mathsf{C}} + \mathcal{L}_z^{\mathsf{rel}}\,. \tag{3.58}$$

The operator $b = \frac{1}{\sqrt{N}} \sum_i a_i$ and its adjoint $b^\dagger$ commute with all $a_i - a_j$, $a_i^\dagger - a_j^\dagger$, and thus with the Hamiltonian and with $\mathcal{L}_z^{\mathsf{rel}}$. Clearly, also, $b^\dagger$ raises $\mathcal{L}_z = \sum_i a_i^\dagger a_i$, and thus $\mathcal{L}_z^C$, by 1. $b^\dagger$ and b are thus ladder operators for the center-of-mass part of the angular momentum. From the commutation relation

$$[b, b^\dagger] = 1 \tag{3.59}$$

it follows that $b^\dagger$ cannot annihilate any non-zero ket of the Hilbert space. From the above it thus follows that the entire spectrum $\Sigma_{\mathcal{L}_z}$ for a given value of $\mathcal{L}_z$ is contained in that for $\mathcal{L}_z + 1$, $\Sigma_{\mathcal{L}_z+1}$: $b^\dagger$ always raises the value of $\mathcal{L}_z$ while keeping the energy the same. This in particular implies the monotony,

$$E_0(N, \mathcal{L}_z) \geq E_0(N, \mathcal{L}_z + 1)\,. \tag{3.60}$$

The above is simply a manifestation of center-of-mass degeneracy in the infinite plane, and is not too surprising. Note that unlike when using conjugate magnetic translations to establish a similar degeneracy (cf., e.g., Ref. [38]), the equality of the spectra at $\mathcal{L}_z$ and $\mathcal{L}_z + 1$ does not follow, since b can, in general, annihilate non zero kets. However, $\Sigma_{\mathcal{L}_z}$ is identical to the spectrum associated to the subspace having angular momentum $\mathcal{L}_z + 1$ and $\mathcal{L}_z^C > 0$. In determining the full spectrum, it is thus sufficient to focus on the subspaces characterized by $\mathcal{L}_z^C = 0$ and all possible values for $\mathcal{L}_z = \mathcal{L}_z^{\mathsf{rel}}$. A more interesting question is thus whether the ground-state energy $E_0(N, \mathcal{L}_z, \mathcal{L}_z^C = 0)$ as a function of given N, $\mathcal{L}_z$ and subject to the constraint $\mathcal{L}_z^C = 0$ satisfies a monotony similar to Eq. (3.60). We leave detailed analysis as an interesting problem for the future.

We emphasize that the above is true exactly only when no cutoff in orbital space is imposed, other than what naturally follows from fixing total angular momentum (i.e., for bosons, no orbitals with $n > \mathcal{L}_z$ allowed, and a correspondingly lower cutoff for fermions). Since, for example, in numerical calculations the second-quantized framework used throughout most of this chapter may be deemed preferable, we will give second-quantized expressions for the operators b, $b^\dagger$ and the various components of angular momentum appearing in Eq. (3.58).

Clearly, the operators b, $b^\dagger$ are single body operators changing the total angular momentum by ± 1 while preserving energy. In particular, they preserve zero modes of special Hamil-

tonians. This last circumstance allows us to make contact with our recent work [48, 49, 95], where a class of second-quantized single body operators was discussed for various geometries that preserve zero modes. These operators $\mathcal{O}_d$ are labeled by an integer d, and in disk geometry, raise $\mathcal{L}_z$ by d. Up to some arbitrary normalization which we will fix here for our purposes, the operator $\mathcal{O}_1$ for the disk is given by [48]

$$\mathcal{O}_1 = \sum_{n=0}^{\infty} \sqrt{n+1}\, c_{n+1}^\dagger c_n \,. \tag{3.61}$$

It is thus natural to assume that $b^\dagger$ is proportional to this operator. Indeed, the action of $\mathcal{O}_1$ can be seen [48, 95], at first quantized level, to correspond to multiplication of an analytic wave function with a factor proportional to $\sum_{i=1}^N z_i$. Here, $z_i = x_i + iy_i$ as usual. The same can easily be established for the operator $b^\dagger$. Hence up to normalization, these operators are the same. One easily verifies $[\mathcal{O}_1^\dagger, \mathcal{O}_1] = \hat{N}$, such that comparison with Eq. (3.59) gives

$$b^\dagger = \frac{1}{\sqrt{\hat{N}}} \mathcal{O}_1 \,. \tag{3.62}$$

Alternatively, one may verify directly, if desired, that Eq. (3.61) commutes with all Haldane pseudopotentials, and thus only acts on center-of-mass degrees of freedom. The operators for various aspects of angular momentum are then given by

$$\mathcal{L}_z = \sum_{n=0}^{\infty} n\, c_n^\dagger c_n \,, \tag{3.63}$$

which is obvious. Furthermore,

$$\mathcal{L}_z^C = b^\dagger b\,, \tag{3.64}$$

which is, up to terms proportional to particle number, a two-body operator, and $\mathcal{L}_z^{\mathsf{rel}}$ is then obtained from Eq. (3.58).

3.3 Discussion and Conclusion

In this chapter, we have been interested in bounds describing the evolution in particle number of low-energy spectral properties for both general and "special" positive two-body interaction Hamiltonians. Even in the latter, "special" case, we have accessed properties which are beyond the zero mode subspace that renders these Hamiltonians special. We have thus naturally employed a second-quantized framework, which we find superior for addressing any properties not directly related to zero modes, whether or not the latter are present.

Our starting point has been the general monotony of the ground-state energy in particle number, for any positive interaction Hamiltonian. We then asked what additional information can be obtained using strategies related to those used in the proof of this monotony property when additional assumptions applying to a wide class of fractional quantum Hall model Hamiltonians are made. Specifically, we have focused on two-body interactions with center-of-mass conservation. For fermions, in many situations of interest one also has a particle-hole symmetry, and we observed that this alone can be used to immediately translate the monotony property into a general bound on the energy step size, giving in particular an upper bound on the charge gap at the "incompressible filling factor" of special model

Hamiltonians. This bound was subsequently improved and generalized to bosons. We also used a dual argument to obtain similar bounds for the first excited state in the presence of zero modes, thus showing that for special model Hamiltonians possessing the latter, non-trivial statements are possible even for excited states at non zero energy.

While we have been mostly concerned with compact geometries, in particular, the torus and sphere, we have also commented on the situation in the infinite disk geometry, where center-of mass degeneracy leads to an obvious monotony property as a function of angular momentum. In this context, we also commented on aspects of center-of-mass and relative-coordinate decomposition in the framework of second quantization.

We are hopeful that these results will spur further development regarding exact properties beyond zero modes in model Hamiltonians of fractional quantum Hall states and related systems.

BIBLIOGRAPHY

[1] Steven M. Girvin Richard E. Prange, editor. *The Quantum Hall Effect*. Springer New York, 1990.

[2] Allan H Macdonald. Introduction to the physics of the quantum hall regime. *arXiv preprint cond-mat/9410047*, 1994.

[3] Jainendra K. Jain. *Composite Fermions*. Cambridge University Press, 2007. Cambridge Books Online.

[4] E. H. Hall. On a new action of the magnet on electric currents. *American Journal of Mathematics*, 2(3):287–292, 1879.

[5] T Chakraborty and P Pietilainen. The Fractional Quantum Hall Effect, 1988.

[6] Aron Pinczuk and Sankar Das Sarma. *Perspectives in Quantum Hall Effects: Novel Quantum Liquids in Low-Dimensional Semiconductor Structures*. Wiley, 1997.

[7] Michael Stone. *Quantum Hall Effect*. World Scientific, 1992.

[8] K. v. Klitzing, G. Dorda, and M. Pepper. New Method for High-Accuracy Determination of the Fine-Structure Constant Based on Quantized Hall Resistance. *Phys. Rev. Lett.*, 45:494–497, Aug 1980.

[9] L.D. Landau. *Z. Phys.*, 64:623, 1930.

[10] V. Fock. *Z. Phys.*, 47:446, 1928.

[11] John Flavin and Alexander Seidel. Abelian and Non-Abelian Statistics in the Coherent State Representation. *Phys. Rev. X*, 1:021015, Dec 2011.

[12] F. D. M. Haldane. Fractional Quantization of the Hall Effect: A Hierarchy of Incompressible Quantum Fluid States. *Phys. Rev. Lett.*, 51:605–608, Aug 1983.

[13] G. Fano, F. Ortolani, and E. Colombo. Configuration-interaction calculations on the fractional quantum Hall effect. *Phys. Rev. B*, 34:2670–2680, Aug 1986.

[14] R. B. Laughlin. Quantized Hall conductivity in two dimensions. *Phys. Rev. B*, 23:5632–5633, May 1981.

[15] B. I. Halperin. Quantized Hall conductance, current-carrying edge states, and the existence of extended states in a two-dimensional disordered potential. *Phys. Rev. B*, 25:2185–2190, Feb 1982.

[16] R. E. Prange and Robert Joynt. Conduction in a strong field in two dimensions: The quantum Hall effect. *Phys. Rev. B*, 25:2943–2946, Feb 1982.

[17] S. A. Trugman. Localization, percolation, and the quantum Hall effect. *Phys. Rev. B*, 27:7539–7546, Jun 1983.

[18] Rolf Landauer. Electrical resistance of disordered one-dimensional lattices. *Philosophical Magazine*, 21(172):863–867, 1970.

[19] D. C. Tsui, H. L. Stormer, and A. C. Gossard. Two-dimensional magnetotransport in the extreme quantum limit. *Phys. Rev. Lett.*, 48:1559–1562, May 1982.

[20] A. M. Chang, P. Berglund, D. C. Tsui, H. L. Stormer, and J. C. M. Hwang. Higher-Order States in the Multiple-Series, Fractional, Quantum Hall Effect. *Phys. Rev. Lett.*, 53:997–1000, Sep 1984.

[21] V. J. Goldman, M. Shayegan, and D. C. Tsui. Evidence for the Fractional Quantum Hall State at $\nu = \frac{1}{7}$. *Phys. Rev. Lett.*, 61:881–884, Aug 1988.

[22] G Ebert, K Von Klitzing, JC Maan, G Remenyi, C Probst, G Weimann, and W Schlapp. Fractional quantum Hall effect at filling factors up to ν= 3. *Journal of Physics C: Solid State Physics*, 17(29):L775, 1984.

[23] W. Pan, H. L. Stormer, D. C. Tsui, L. N. Pfeiffer, K. W. Baldwin, and K. W. West. Fractional Quantum Hall Effect of Composite Fermions. *Phys. Rev. Lett.*, 90:016801, Jan 2003.

[24] J. P. Eisenstein and H. L. Stormer. The Fractional Quantum Hall Effect. *Science*, 248(4962):1510–1516, 1990.

[25] Lev Davidovich Landau and VL Ginzburg. On the theory of superconductivity. *Zh. Eksp. Teor. Fiz.*, 20:1064, 1950.

[26] Dirk Ter Haar. *Collected papers of LD Landau*. Elsevier, 2013.

[27] Xiao-Gang Wen. Topological orders and edge excitations in fractional quantum Hall states. *Advances in Physics*, 44(5):405–473, 1995.

[28] Xiao-Gang Wen. Quantum field theory of many-body systems: from the origin of sound to an origin of light and electrons, 2004.

[29] Xiao-Gang Wen. Continuous topological phase transitions between clean quantum Hall states. *Physical review letters*, 84(17):3950, 2000.

[30] Xiao-Gang Wen. Topological orders in rigid states. *International Journal of Modern Physics B*, 4(02):239–271, 1990.

[31] Michael Levin and Xiao-Gang Wen. Detecting topological order in a ground state wave function. *Physical review letters*, 96(11):110405, 2006.

[32] VJ Goldman and Bo Su. Resonant tunneling in the quantum Hall regime: measurement of fractional charge. *Science*, 267(5200):1010, 1995.

[33] R. B. Laughlin. Anomalous Quantum Hall Effect: An Incompressible Quantum Fluid with Fractionally Charged Excitations. *Phys. Rev. Lett.*, 50:1395–1398, May 1983.

[34] Steven H. Simon, E. H. Rezayi, and Nigel R. Cooper. Pseudopotentials for multiparticle interactions in the quantum hall regime. *Phys. Rev. B*, 75:195306, May 2007.

[35] B. Estienne, Z. Papić, N. Regnault, and B. A. Bernevig. Matrix product states for trial quantum Hall states. *Phys. Rev. B*, 87:161112, Apr 2013.

[36] Michael P. Zaletel and Roger S. K. Mong. Exact matrix product states for quantum Hall wave functions. *Phys. Rev. B*, 86:245305, Dec 2012.

[37] B. Andrei Bernevig and F. D. M. Haldane. Model Fractional Quantum Hall States and Jack Polynomials. *Phys. Rev. Lett.*, 100:246802, Jun 2008.

[38] Alexander Seidel, Henry Fu, Dung-Hai Lee, Jon Magne Leinaas, and Joel Moore. Incompressible Quantum Liquids and New Conservation Laws. *Phys. Rev. Lett.*, 95:266405, Dec 2005.

[39] Alexander Seidel and Dung-Hai Lee. Abelian and Non-Abelian Hall Liquids and Charge-Density Wave: Quantum Number Fractionalization in One and Two Dimensions. *Phys. Rev. Lett.*, 97:056804, Aug 2006.

[40] Alexander Seidel and Kun Yang. Halperin $(m, m^{'}, n)$ bilayer quantum hall states on thin cylinders. *Phys. Rev. Lett.*, 101:036804, Jul 2008.

[41] Alexander Seidel. Pfaffian Statistics through Adiabatic Transport in the 1D Coherent State Representation. *Phys. Rev. Lett.*, 101:196802, Nov 2008.

[42] Gregory Moore and Nicholas Read. Nonabelions in the fractional quantum Hall effect. *Nuclear Physics B*, 360(23):362 – 396, 1991.

[43] Xiao-Gang Wen. Theory of the edge states in fractional quantum Hall effects. *International Journal of Modern Physics B*, 06(10):1711–1762, 1992.

[44] Edward Witten. Quantum field theory and the Jones polynomial. *Communications in Mathematical Physics*, 121(3):351–399, 1989.

[45] Willem Hendrik Dickhoff and Dimitri Van Neck. *Many-body theory exposed!: propagator description of quantum mechanics in many-body systems*. World Scientific, 2008.

[46] Henrik Bruus and Karsten Flensberg. *Many-body quantum theory in condensed matter physics: an introduction*. Oxford University Press, 2004.

[47] Alexander Seidel and Kun Yang. Gapless excitations in the Haldane-Rezayi state: The thin-torus limit. *Physical Review B*, 84(8):085122, 2011.

[48] G. Ortiz, Z. Nussinov, J. Dukelsky, and A. Seidel. Repulsive interactions in quantum Hall systems as a pairing problem. *Phys. Rev. B*, 88:165303, Oct 2013.

[49] Li Chen and Alexander Seidel. Algebraic approach to the study of zero modes of Haldane pseudopotentials. *Phys. Rev. B*, 91:085103, Feb 2015.

[50] R. L. Willett, M. A. Paalanen, R. R. Ruel, K. W. West, L. N. Pfeiffer, and D. J. Bishop. Anomalous sound propagation at ν=1/2 in a 2D electron gas: Observation of a spontaneously broken translational symmetry? *Phys. Rev. Lett.*, 65:112–115, Jul 1990.

[51] B. I. Halperin, Patrick A. Lee, and Nicholas Read. Theory of the half-filled Landau level. *Phys. Rev. B*, 47:7312–7343, Mar 1993.

[52] Dam Thanh Son. Is the Composite Fermion a Dirac Particle? *Phys. Rev. X*, 5:031027, Sep 2015.

[53] Chong Wang and T. Senthil. Half-filled Landau level, topological insulator surfaces, and three-dimensional quantum spin liquids. *Phys. Rev. B*, 93:085110, Feb 2016.

[54] F. D. M. Haldane. Geometrical Description of the Fractional Quantum Hall Effect. *Phys. Rev. Lett.*, 107:116801, Sep 2011.

[55] Amila Weerasinghe and Alexander Seidel. Thin torus perturbative analysis of elementary excitations in the Gaffnian and Haldane-Rezayi quantum Hall states. *Phys. Rev. B*, 90:125146, Sep 2014.

[56] Amila Weerasinghe, Tahereh Mazaheri, and Alexander Seidel. Bounds for low-energy spectral properties of center-of-mass conserving positive two-body interactions. *Phys. Rev. B*, 93:155135, Apr 2016.

[57] Steven H. Simon, E. H. Rezayi, N. R. Cooper, and I. Berdnikov. Construction of a paired wave function for spinless electrons at filling fraction $\nu = 25$. *Phys. Rev. B*, 75:075317, Feb 2007.

[58] F. D. M. Haldane and E. H. Rezayi. Spin-singlet wave function for the half-integral quantum Hall effect. *Phys. Rev. Lett.*, 60:956–959, Mar 1988.

[59] N. Read. Non-Abelian adiabatic statistics and Hall viscosity in quantum Hall states and px+ipy paired superfluids. *Phys. Rev. B*, 79:045308, Jan 2009.

[60] N. Read. Conformal invariance of chiral edge theories. *Phys. Rev. B*, 79:245304, Jun 2009.

[61] N. Read and Dmitry Green. Paired states of fermions in two dimensions with breaking of parity and time-reversal symmetries and the fractional quantum Hall effect. *Phys. Rev. B*, 61:10267–10297, Apr 2000.

[62] Yuan-Ming Lu, Xiao-Gang Wen, Zhenghan Wang, and Ziqiang Wang. Non-Abelian quantum Hall states and their quasiparticles: From the pattern of zeros to vertex algebra. *Phys. Rev. B*, 81:115124, Mar 2010.

[63] N. Regnault, B. A. Bernevig, and F. D. M. Haldane. Topological Entanglement and Clustering of Jain Hierarchy States. *Phys. Rev. Lett.*, 103:016801, Jun 2009.

[64] B Andrei Bernevig, Parsa Bonderson, and Nicolas Regnault. Screening Behavior and Scaling Exponents from Quantum Hall Wavefunctions. *arXiv:1207.3305*, 2012.

[65] Th. Jolicoeur, T. Mizusaki, and Ph. Lecheminant. Absence of a gap in the Gaffnian state. *Phys. Rev. B*, 90:075116, Aug 2014.

[66] John Flavin, Ronny Thomale, and Alexander Seidel. Gaffnian holonomy through the coherent state method. *Phys. Rev. B*, 86:125316, Sep 2012.

[67] E. J. Bergholtz and A. Karlhede. Half-Filled Lowest Landau Level on a Thin Torus. *Phys. Rev. Lett.*, 94:26802, 2005.

[68] Emil J Bergholtz and Anders Karlhede. 'one-dimensional' theory of the quantum hall system. *Journal of Statistical Mechanics: Theory and Experiment*, 2006(04):L04001, 2006.

[69] E. J. Bergholtz, J. Kailasvuori, E. Wikberg, T. H. Hansson, and A. Karlhede. Pfaffian quantum Hall state made simple: Multiple vacua and domain walls on a thin torus. *Phys. Rev. B*, 74:081308, Aug 2006.

[70] Alexander Seidel. S -Duality Constraints on 1D Patterns Associated with Fractional Quantum Hall States. *Phys. Rev. Lett.*, 105:026802, Jul 2010.

[71] Alexander Seidel and Dung-Hai Lee. Domain-wall-type defects as anyons in phase space. *Phys. Rev. B*, 76:155101, Oct 2007.

[72] Emil Johansson Bergholtz, Janik Kailasvuori, Emma Wikberg, Thors Hans Hansson, and Anders Karlhede. Pfaffian quantum Hall state made simple: Multiple vacua and domain walls on a thin torus. *Physical Review B*, 74(8):081308, 2006.

[73] Esko Keski-Vakkuri and Xiao-Gang Wen. The Ground state structure and modular transformations of fractional quantum Hall states on a torus. *International Journal of Modern Physics B*, 7(25):4227–4259, 1993.

[74] Dung-Hai Lee and Jon Magne Leinaas. Mott Insulators without Symmetry Breaking. *Phys. Rev. Lett.*, 92:096401, Mar 2004.

[75] N. Read and E. Rezayi. Quasiholes and fermionic zero modes of paired fractional quan-

tum Hall states: The mechanism for non-Abelian statistics. *Phys. Rev. B*, 54:16864–16887, Dec 1996.

[76] Michael Reed and Barry Simon. *Methods of modern mathematical physics, Scattering theory*, volume III. Academic Press, New York, 1979.

[77] Steven H Simon, EH Rezayi, and Nigel R Cooper. Generalized quantum Hall projection hamiltonians. *Physical Review B*, 75(7):075318, 2007.

[78] Ching Hua Lee, Ronny Thomale, and Xiao-Liang Qi. Pseudopotential formalism for fractional Chern insulators. *Phys. Rev. B*, 88:035101, Jul 2013.

[79] Xia-Gang Wen and Yong-Shi Wu. Chiral operator product algebra hidden in certain fractional quantum Hall wave functions. *Nuclear Physics B*, 419(3):455–479, 1994.

[80] N. Read and E. Rezayi. Beyond paired quantum Hall states: Parafermions and incompressible states in the first excited Landau level. *Phys. Rev. B*, 59:8084–8092, Mar 1999.

[81] B. Andrei Bernevig and F. D. M. Haldane. Generalized clustering conditions of Jack polynomials at negative Jack parameter α. *Phys. Rev. B*, 77:184502, May 2008.

[82] G. C. Wick. The Evaluation of the Collision Matrix. *Phys. Rev.*, 80:268–272, Oct 1950.

[83] Xiao-Liang Qi. Generic Wave-Function Description of Fractional Quantum Anomalous Hall States and Fractional Topological Insulators. *Phys. Rev. Lett.*, 107:126803, Sep 2011.

[84] Z. Papić. Solvable models for unitary and nonunitary topological phases. *Phys. Rev. B*, 90:075304, Aug 2014.

[85] Abolhassan Vaezi and Maissam Barkeshli. Fibonacci Anyons From Abelian Bilayer Quantum Hall States. *Phys. Rev. Lett.*, 113:236804, Dec 2014.

[86] B. I. Halperin. Statistics of Quasiparticles and the Hierarchy of Fractional Quantized Hall States. *Phys. Rev. Lett.*, 52:1583–1586, Apr 1984.

[87] S. A. Trugman and S. Kivelson. Exact results for the fractional quantum Hall effect with general interactions. *Phys. Rev. B*, 31:5280–5284, Apr 1985.

[88] J. Dubail, N. Read, and E. H. Rezayi. Edge-state inner products and real-space entanglement spectrum of trial quantum Hall states. *Physical Review B*, 86(24):245310, December 2012.

[89] DN Sheng, Zheng-Cheng Gu, Kai Sun, and L Sheng. Fractional quantum Hall effect in the absence of Landau levels. *Nature communications*, 2:389, 2011.

[90] Titus Neupert, Luiz Santos, Claudio Chamon, and Christopher Mudry. Fractional Quantum Hall States at Zero Magnetic Field. *Phys. Rev. Lett.*, 106:236804, Jun 2011.

[91] N. Regnault and B. Andrei Bernevig. Fractional Chern Insulator. *Phys. Rev. X*, 1:021014, Dec 2011.

[92] Evelyn Tang, Jia-Wei Mei, and Xiao-Gang Wen. High-Temperature Fractional Quantum Hall States. *Phys. Rev. Lett.*, 106:236802, Jun 2011.

[93] T. Scaffidi and S. H. Simon. Exact Solutions of Fractional Chern Insulators: Interacting Particles in the Hofstadter Model at Finite Size. *Phys. Rev. B*, 90:115132, July 2014.

[94] Li Chen, Tahereh Mazaheri, Alexander Seidel, and Xiang Tang. The impossibility of exactly flat non-trivial Chern bands in strictly local periodic tight binding models. *Journal of Physics A: Mathematical and Theoretical*, 47(15):152001, 2014.

[95] Tahereh Mazaheri, Gerardo Ortiz, Zohar Nussinov, and Alexander Seidel. Zero modes, bosonization, and topological quantum order: The Laughlin state in second quantization. *Phys. Rev. B*, 91:085115, Feb 2015.

[96] Ching Hua Lee, Zlatko Papić, and Ronny Thomale. Geometric Construction of Quantum Hall Clustering Hamiltonians. *Phys. Rev. X*, 5:041003, Oct 2015.

[97] ElliottH. Lieb. The Bose Gas: A Subtle Many-Body Problem. In Walter Thirring, editor, *The Stability of Matter: From Atoms to Stars*, pages 699–719. Springer Berlin Heidelberg, 2001.

[98] Gunnar Möller and Steven H. Simon. Composite fermions in a negative effective magnetic field: A Monte Carlo study. *Phys. Rev. B*, 72:045344, Jul 2005.

[99] S. M. Girvin, A. H. MacDonald, and P. M. Platzman. Collective-Excitation Gap in the Fractional Quantum Hall Effect. *Phys. Rev. Lett.*, 54:581–583, Feb 1985.

[100] S. M. Girvin, A. H. MacDonald, and P. M. Platzman. Magneto-roton theory of col-

lective excitations in the fractional quantum Hall effect. *Phys. Rev. B*, 33:2481–2494, Feb 1986.